

Gaussian Copula Models for Nonignorable Missing Data Using Auxiliary Marginal Quantiles

Joseph Feldman¹, Jerome P. Reiter¹, and Daniel R. Kowal*^{2,3}

¹Department of Statistical Science, Duke University

²Department of Statistics and Data Science, Cornell University

³Department of Statistics, Rice University

June 6, 2024

Abstract

We present an approach for modeling and imputation of nonignorable missing data under Gaussian copulas. The analyst posits a set of quantiles of the marginal distributions of the study variables, for example, reflecting information from external data sources or elicited expert opinion. When these quantiles are accurately specified, we prove it is possible to consistently estimate the copula correlation and perform multiple imputation in the presence of nonignorable missing data. We develop algorithms for estimation and imputation that are computationally efficient, which we evaluate in simulation studies of multiple imputation inferences. We apply the model to analyze associations between lead exposure levels and end-of-grade test scores for 170,000 students in North Carolina. These measurements are not missing at random, as children deemed at-risk for high lead exposure are more likely to be measured. We construct plausible marginal quantiles for lead exposure using national statistics provided by the Centers for Disease Control and Prevention. Complete cases and missing at random analyses appear to underestimate the relationships between certain variables and end-of-grade test scores, while multiple imputation inferences under our model support stronger, adverse associations between lead exposure and educational outcomes.

Keywords: Bayesian; imputation; MNAR; data integration; nonresponse

*The findings and conclusions in this paper are those of the authors and do not necessarily represent the views of the North Carolina Department of Health and Human Services, Division of Public Health

1 Introduction

The Gaussian copula is a flexible joint distribution for multivariate data. The model can characterize complex dependencies while also capturing non-Gaussian marginal distributions. Methodological advances have made the Gaussian copula compatible with mixed data types (Hoff, 2007; Feldman and Kowal, 2022), increased its scalability to high-dimensional variable sets (Murray et al., 2013), and improved its ability to capture non-linearity and interactions (Feldman and Kowal, 2024). Because of these appealing features, it has been deployed in numerous applications including, for example, in economics and finance (Fan and Patton, 2014), marketing and management (Eckert and Hohberger, 2023), and political science (Chiba et al., 2015).

The Gaussian copula can be readily implemented when data have missing values. Indeed, researchers (e.g., Käärik and Käärik, 2010; Di Lascio et al., 2015; Zhao and Udell, 2020; Hollenbach et al., 2021; Hoff, 2022; Christoffersen et al., 2023) have suggested Gaussian copulas as multivariate, joint modeling engines for (multiple) imputation. Existing methods, however, tend to assume that missingness among the study variables is missing completely at random (MCAR) or missing at random (MAR) (Rubin, 1976). We are not aware of methodology for itemwise nonignorable missingness with Gaussian copula models.

In this article, we develop a framework to handle nonignorable missing data in Gaussian copula models. Our general strategy is to specify a Bayesian Gaussian copula model that includes both the study variables and the missingness indicators, coupled with auxiliary information on the marginal distributions of the study variables. Using this strategy, we prove that analysts need to know only a small, arbitrary set of auxiliary marginal quantiles to enable consistent estimation of the copula correlation; entire distributions are not necessary. These results hold for a version of an additive nonignorable (AN) missingness

mechanism (Hirano et al., 2001; Sadinle and Reiter, 2019). This mechanism allows the reason for missingness in a variable potentially to depend on the value of the variable itself. We develop algorithms for estimating the copula correlation that result in significant computational gains relative to alternative copula models, which allows fitting to scale to data with (moderately) large sample sizes in reasonable time using typical computational setups. We also present strategies for estimating other quantiles of the marginal distributions beyond those in the auxiliary information. Our approach provides uncertainty quantification for the unknown marginals, which we utilize for multiple imputation (Rubin, 1987).

We develop the methodology for settings where marginal quantiles for variables subject to missingness are available in external data sources. For example, previewing the application in Section 5, suppose an analysis involving health measurements suffers from nonignorable missingness, e.g., people likely to have uncerning values are not measured. For many health measurements, there exists information on marginal quantiles from national benchmark surveys or administrative databases. We seek to use the auxiliary quantiles to adjust for nonignorable missingness in the analysis at hand. When auxiliary quantiles are not available or known precisely, analysts can posit different plausible marginal quantiles and assess the sensitivity of ultimate analyses under those specifications, e.g., via multiple imputation analyses. We note that the use of known marginal distributions for imputation of nonignorable missing data also has been proposed for categorical data models (Pham et al., 2018; Akande et al., 2021; Deng et al., 2013; Si et al., 2015, 2016; Tang et al., 2024), but not for continuous and mixed variables like we do here.

We apply the methodology in data comprising health, socioeconomic, demographic and educational measurements collected on over 170,000 North Carolina children. Among the study variables are end-of-grade math and reading test scores and a measure of lead

exposure, the latter of which is subject to abundant missingness that is likely nonignorable. The state requires children at high risk of lead exposure to be measured, but not children at low risk of lead exposure. To inform the imputation of the missing values, we leverage marginal quantiles on lead exposure published by the Centers for Disease Control and Prevention. Using this information, we find lead exposure apparently is more adversely associated with test scores than suggested from complete cases or MAR analyses.

The remainder of this article is organized as follows. In Section 2, we present the Gaussian copula model with nonignorable missing data and information on marginal distributions. Here we present two theoretical results, namely (i) that fully specified marginal distributions provide posterior consistency of the copula correlation in the presence of non-ignorable missingness, and (ii) a derivation that the Gaussian copula implies a version of the AN missingness mechanism. In Section 3, we modify the copula model and develop imputation strategies for settings where the auxiliary marginal information constitutes a specified set of marginal quantiles. Here we present our main theorem: under the AN missingness mechanism, this limited auxiliary information still allows consistent estimation of the copula correlation. In Section 4, we present simulations studying the effect of differing amounts of auxiliary quantiles and repeated sampling properties of multiple imputation inferences with the model. In Section 5, we present the analysis of the North Carolina lead exposure data. In Section 6, we summarize and suggest research directions. Codes for all analyses are available at <https://github.com/jfeldman396/EHQL-Impute>.

2 Gaussian Copula with Nonignorable Missing Data

For $i = 1, \dots, n$ individuals, let $\mathbf{y}_i = (y_{i1}, \dots, y_{ip})$ comprise measurements on p study variables. Let $\mathbf{y} = \{\mathbf{y}_i : i = 1, \dots, n\}$. When \mathbf{y} contains missing values, let $r_{ij} = 1$ when y_{ij} is missing, and $r_{ij} = 0$ otherwise. Let $\mathbf{r}_i = \{r_{i1}, \dots, r_{ip}\}$ for $i = 1, \dots, n$, and

$\mathbf{r} = \{\mathbf{r}_i : i = 1, \dots, n\}$. We refer to the study variables using $Y = (Y_1, \dots, Y_p)$ and nonresponse indicators using $R = (R_1, \dots, R_p)$. When the missingness is nonignorable, we require a model for the joint distribution of (\mathbf{y}, \mathbf{r}) . To aid specification of this distribution, we partition the data into observed and missing components, $\mathbf{y} = (\mathbf{y}^{obs}, \mathbf{y}^{mis})$, where $\mathbf{y}^{obs} = \{y_{ij} : r_{ij} = 0; i = 1, \dots, n; j = 1, \dots, p\}$ and $\mathbf{y}^{mis} = \{y_{ij} : r_{ij} = 1; i = 1, \dots, n; j = 1, \dots, p\}$. Then, the two principal modeling tasks are to specify the distribution of the observed data,

$$p(\mathbf{y}^{obs}, \mathbf{r} | \boldsymbol{\gamma}) = \int p(\mathbf{y}^{obs}, \mathbf{y}^{mis}, \mathbf{r} | \boldsymbol{\gamma}) d\mathbf{y}^{mis}, \quad (1)$$

and to impose some identifying restriction on $p(\mathbf{y}^{mis} | \mathbf{y}^{obs}, \mathbf{r}, \boldsymbol{\gamma})$, also known as the extrapolation model (Linero and Daniels, 2018). Here, $\boldsymbol{\gamma}$ are parameters of the model for (\mathbf{y}, \mathbf{r}) . We accomplish these tasks via a Gaussian copula specification, which we now describe.

For each $(\mathbf{y}_i, \mathbf{r}_i)$, let $\mathbf{z}_i = (\mathbf{z}_{\mathbf{y}_i}, \mathbf{z}_{\mathbf{r}_i})$ be a $2p \times 1$ vector of latent variables. Here, $\mathbf{z}_{\mathbf{y}_i} = (z_{i1}, \dots, z_{ip})$ and $\mathbf{z}_{\mathbf{r}_i} = (z_{i(p+1)}, \dots, z_{i(2p)})$. Let $\boldsymbol{\alpha} = (\mathbf{0}_p, \alpha_{r_1}, \dots, \alpha_{r_p})$ be a $2p \times 1$ vector, where $\mathbf{0}_p$ is a vector of p zeros corresponding to $\mathbf{z}_{\mathbf{y}_i}$ and the next p elements correspond to $\mathbf{z}_{\mathbf{r}_i}$. Let $\mathbf{C}_{\boldsymbol{\theta}}$ be a $2p \times 2p$ copula correlation matrix. With generality, we let $\boldsymbol{\theta}$ include parameters that generate a copula correlation; see Section 4 for the specification in our analyses. For $j = 1, \dots, p$, let F_j be the marginal distribution for Y_j . To begin, we assume that each Y_j is continuous; modifications for discrete Y_j are introduced in Section 3. To incorporate unordered categorical variables, we employ the construction in Feldman and Kowal (2022); see the supplement for details. The data generating model is then

$$\mathbf{z}_i \sim N_{2p}(\boldsymbol{\alpha}, \mathbf{C}_{\boldsymbol{\theta}}) \quad (2)$$

$$y_{ij} = F_j^{-1}\{\Phi(z_{y_{ij}})\}; \quad r_{ij} = \mathbb{1}_{z_{i(p+j)} > 0}, \quad (3)$$

where $\mathbb{1}_e = 1$ when the expression e in its index is true and $\mathbb{1}_e = 0$ otherwise. The $\mathbf{C}_{\boldsymbol{\theta}}$ captures multivariate dependence among the study variables themselves as well as between

study variables and nonresponse indicators. The values of $(\alpha_{r_1}, \dots, \alpha_{r_p})$ model the marginal probabilities of missingness. For the study variables, each z_{ij} is transformed to the observed data scale by applying the standard normal cumulative distribution function Φ and the inverse of the marginal distribution function for Y_j . For the nonresponse indicators, each $z_{i(p+j)}$ satisfies a probit data augmentation (Chib and Greenberg, 1998).

For prediction or imputation under copula models with no missing or MCAR data, analysts typically estimate each F_j from \mathbf{y}^{obs} using the empirical CDF (Hoff, 2007; Feldman and Kowal, 2022; Zhao and Udell, 2020) or with some model (Pitt et al., 2006; Feldman and Kowal, 2024). With nonignorable missing data, however, estimates of $\{F_j\}_{j=1}^p$ computed from \mathbf{y}^{obs} can be biased, which in turn affects the quality of imputations of \mathbf{y}^{mis} . Additionally, inference for \mathbf{C}_θ from $(\mathbf{y}^{obs}, \mathbf{r})$ alone may be biased, as we show in Section 4.

We address these potential problems by utilizing some source of auxiliary information about each F_j . We write this auxiliary information set as \mathcal{A}_j and, across study variables, as $\mathcal{A} = \{\mathcal{A}_j\}_{j=1}^p$. As a first step, we presume $\mathcal{A}_j = F_j$ for all j , i.e., the full marginal distributions are known. In this case, we show that \mathbf{C}_θ can be consistently estimated despite the presence of nonignorable missing data (Section 2.1) and that the Gaussian copula implies a version of an AN missingness mechanism (Section 2.2). We leverage these results in Section 3 when \mathcal{A} comprises quantiles rather than full distributions.

In what follows, we include an R_j for each Y_j in the modeling. When Y_j is considered MCAR or has no missing values, analysts can remove R_j from (2) and (3), which reduces the dimension of \mathbf{z}_i .

2.1 Results with Complete Marginals

Let $\mathbf{z}_y = \{\mathbf{z}_{y_i} : i = 1, \dots, n\}$ and $\mathbf{z}_r = \{\mathbf{z}_{r_i} : i = 1, \dots, n\}$ be the collections of latent variables for the study variables and nonresponse indicators, respectively. For convenience,

we partition $\mathbf{z}_y = (\mathbf{z}^{obs}, \mathbf{z}^{mis})$ into observed and missing components corresponding to $(\mathbf{y}^{obs}, \mathbf{y}^{mis})$. Define the set restriction $\mathcal{E}(\mathbf{r})$ as the condition that \mathbf{z}_r satisfies the probit constraints in (3) for the realized \mathbf{r} across $i = 1, \dots, n$ and $j = p + 1, \dots, 2p$. Because each F_j is known from \mathcal{A} , the latent variable corresponding to each y_{ij}^{obs} is fixed to $z_{ij}^{obs} = \Phi^{-1}\{F_j(y_{ij}^{obs})\}$. Thus, by conditioning on $\{F_j\}_{j=1}^p$, (1) becomes

$$p(\mathbf{y}^{obs}, \mathbf{r} \mid \mathbf{C}_\theta, \boldsymbol{\alpha}, \{F_j\}_{j=1}^p) = p\{\mathbf{z}^{obs}, \mathbf{z}_r \in \mathcal{E}(\mathbf{r}) \mid \mathbf{C}_\theta, \boldsymbol{\alpha}\} \quad (4)$$

$$= \int \int_{\mathbf{z}_r \in \mathcal{E}(\mathbf{r})} \phi_{2p}(\mathbf{z}^{obs}, \mathbf{z}^{mis}, \mathbf{z}_r; \mathbf{C}_\theta, \boldsymbol{\alpha}) d\mathbf{z}_r d\mathbf{z}^{mis}, \quad (5)$$

where ϕ_{2p} is the density of a $2p$ -dimensional multivariate normal distribution with covariance \mathbf{C}_θ and mean $\boldsymbol{\alpha}$.

With nonignorable missing data, typically one cannot estimate model parameters consistently unless one knows the full distribution of \mathbf{y}^{mis} . However, as we show in Theorem 1, we need far less information when data follow a copula model: knowledge of the true $\{F_j\}_{j=1}^p$ is sufficient information to ensure consistent estimation of the copula correlation. For a fixed sample $(\mathbf{y}^{obs}, \mathbf{r})$, the posterior distribution of $(\mathbf{C}_\theta, \boldsymbol{\alpha})$ with known marginals is

$$p(\mathbf{C}_\theta, \boldsymbol{\alpha} \mid \mathbf{y}^{obs}, \mathbf{r}, \{F_j\}_{j=1}^p) \propto p(\mathbf{z}^{obs}, \mathbf{z}_r \in \mathcal{E}(\mathbf{r}) \mid \mathbf{C}_\theta, \boldsymbol{\alpha}) p(\mathbf{C}_\theta, \boldsymbol{\alpha}). \quad (6)$$

Subsequently, we refer to the marginal posterior of \mathbf{C}_θ as $\Pi_n(\mathbf{C}_\theta)$.

Theorem 1. *Suppose $\{(\mathbf{y}_i, \mathbf{r}_i)\}_{i=1}^n \stackrel{iid}{\sim} \Pi_0$ where Π_0 is the Gaussian copula with correlation \mathbf{C}_0 and marginals $\{F_j\}_{j=1}^p$ as in (2)–(3), and $\{\mathcal{A}_j\}_{j=1}^p = \{F_j\}_{j=1}^p$. Let $p(\boldsymbol{\theta})$ be a prior with respect a measure that induces a prior Π over the space of all $2p \times 2p$ correlation matrices \mathbb{C} with $\Pi(\mathbf{C}_\theta) > 0$ for all $\mathbf{C}_\theta \in \mathbb{C}$. Then, for all $\epsilon > 0$, $\lim_{n \rightarrow \infty} \Pi_n\{\mathcal{U}_\epsilon(\mathbf{C}_0)\} \rightarrow 1$ almost surely $[\Pi_0]$, where $\mathcal{U}_\epsilon(\mathbf{C}_0) = \{\mathbf{C}_\theta \in \mathbb{C} : \|\mathbf{C}_0 - \mathbf{C}_\theta\|_F < \epsilon\}$ and $\|\cdot\|_F$ is the Frobenius norm.*

The proof is in the supplement. Theorem 1 implies that the copula correlation can be estimated consistently using the observed data $(\mathbf{y}^{obs}, \mathbf{r})$. As a result, we can use the

true $\{F_j\}_{j=1}^p$ and estimates of \mathbf{C}_θ to impute \mathbf{y}^{mis} from (2)–(3). Furthermore, if $\{F_j\}_{j=1}^p$ is not known, Theorem 1 suggests that analysts can specify different $\{F_j\}_{j=1}^p$ to enable interpretable sensitivity analyses. In other words, when the specified $\{F_j\}_{j=1}^p$ is true, analysts are assured that the model estimates the \mathbf{C}_0 that accords with those marginals consistently.

2.2 Implied Additive Nonignorable Missingness Mechanism

The Gaussian copula with known margins implies a specific nonignorable missingness mechanism, $p(R_{ij} = 1 \mid \mathbf{y}^{obs}, \mathbf{y}^{mis}, \mathbf{C}_\theta, \boldsymbol{\alpha}, \{F_j\}_{j=1}^p)$. To show this, we first note that when (Y, R) are distributed according (2)–(3), any subset of these variables also follows a Gaussian copula (Joe, 2014). For the joint distribution of (Y, R_j) , let the corresponding $(p+1) \times (p+1)$ copula correlation matrix be \mathbf{C}_j^* . This comprises the $p \times p$ sub-matrix \mathbf{C}_y of \mathbf{C}_θ corresponding to the study variables concatenated with the $(p+1) \times 1$ column vector $(\mathbf{C}_{\mathbf{y}r_j}, 1)^t$ and $1 \times (p+1)$ row vector $(\mathbf{C}_{r_j\mathbf{y}}, 1)$. Here, $\mathbf{C}_{\mathbf{y}r_j}$ comprises the entries of \mathbf{C}_θ in the column for R_j , and $\mathbf{C}_{r_j\mathbf{y}}$ is its transpose. We have

$$p(R_{ij} = 1 \mid \mathbf{y}^{obs}, \mathbf{y}^{mis}, \mathbf{C}_\theta, \boldsymbol{\alpha}, \{F_j\}_{j=1}^p) = p(R_{ij} = 1 \mid \mathbf{y}_i^{obs}, \mathbf{y}_i^{mis}, \mathbf{C}_j^*, \alpha_{r_j}, \{F_j\}_{j=1}^p) \quad (7)$$

$$= p(Z_{r_{ij}} > 0 \mid \mathbf{z}_i^{obs}, \mathbf{z}_i^{mis}, \mathbf{C}_j^*, \alpha_{r_j}) = 1 - \Phi_{\alpha_{r_j}^*, \sigma_j^{2*}}(0), \quad (8)$$

where $\Phi_{\alpha_{r_j}^*, \sigma_j^{2*}}$ is the CDF of a Gaussian distribution with mean and variance

$$\alpha_{r_j}^* = \alpha_{r_j} + \mathbf{C}_{r_j\mathbf{y}} \mathbf{C}_y^{-1} (\mathbf{z}_i^{obs}, \mathbf{z}_i^{mis}), \quad \sigma_j^{2*} = 1 - \mathbf{C}_{r_j\mathbf{y}} \mathbf{C}_y^{-1} \mathbf{C}_{\mathbf{y}r_j}. \quad (9)$$

Therefore, the marginal missingness mechanism is a probit regression on $(\mathbf{z}_i^{obs}, \mathbf{z}_i^{mis})$.

The expression for $\alpha_{r_j}^*$ reveals a connection to the additive nonignorable (AN) missingness mechanism. For any generic observation $\mathbf{x}_i = (x_{i1}, \dots, x_{ip})$ comprising observed and missing components $(\mathbf{x}_i^{obs}, \mathbf{x}_i^{mis})$, the AN missingness mechanism holds for some X_j when

$$p(R_{ij} = 1 \mid \mathbf{x}_i^{obs}, \mathbf{x}_i^{mis}) = g\left(\beta_0 + \sum_{k=1}^p \beta_k x_{ik}\right), \quad (10)$$

with g satisfying $\lim_{\beta_0 \rightarrow -\infty} g(\beta_0) = 0$ and $\lim_{\beta_0 \rightarrow \infty} g(\beta_0) = 1$. Special cases of AN missingness mechanisms include an itemwise conditionally independent nonresponse (Sadinle and Reiter, 2017) mechanism when $\beta_j = 0$, and a MCAR mechanism when $\beta_k = 0$ for all $k = 1, \dots, p$. Common link functions g include the logistic and probit (Hirano et al., 2001).

Lemma 1 formally connects the model for R_{ij} in (8) to the AN missingness mechanism in (10). Unlike the formulation in Hirano et al. (2001), the AN missingness mechanism for the Gaussian copula model has additivity on the latent scale.

Lemma 1. *Suppose $\{(\mathbf{y}_i, \mathbf{r}_i)\}_{i=1}^n \stackrel{iid}{\sim} \Pi_0$ where Π_0 is the Gaussian copula with correlation \mathbf{C}_0 and marginals $\{F_j\}_{j=1}^p$ as in (2)–(3), and $\{\mathcal{A}_j\}_{j=1}^p = \{F_j\}_{j=1}^p$. For any value of $(\mathbf{y}_i^{obs}, \mathbf{y}_i^{mis})$, $p(R_{ij} = 1 \mid \mathbf{y}_i^{obs}, \mathbf{y}_i^{mis}, \mathbf{C}_j^*, \alpha_{r_j}, \{F_j\}_{j=1}^p)$ satisfies (10) with $x_{ik} = z_{ik}$, g the probit link function in (8)–(9), $\beta_0 = \alpha_{r_j}$, and β_k the k th component of the vector $\mathbf{C}_{r_j \mathbf{y}} \mathbf{C}_{\mathbf{y}}^{-1}$.*

Of course, it is generally impossible to determine whether any specific missingness mechanism holds in practice (Molenberghs et al., 2008). However, if additive nonignorability on the latent scale does not hold, e.g., the true model for z_{r_j} includes interactions between z_j and other latent variables, the Gaussian copula with fixed margins may not offer reliable inferences or sensitivity analyses. Developing methods and sensitivity analyses for nonignorable missingness that is not AN are topics for future research

3 Using Auxiliary Quantiles

In many contexts, the available information on the marginals does not comprise full distributions. For example, analysts may have access to sets of quantiles from other data sources but not entire distributions. Or, they may be able to elicit reasonable marginal quantiles of F_j from domain experts but not necessarily an entire distribution. To incorporate this information within the Gaussian copula framework, we address two salient issues. First, with incomplete knowledge of any F_j , the transformation between y_{ij} and z_{ij} is un-

known, which could complicate estimation of \mathbf{C}_θ . Second, a small set of auxiliary quantiles for each study variable could be insufficient for imputation of \mathbf{y}^{mis} .

For each Y_j , suppose we have a finite set of $m_j \geq 3$ non-decreasing quantiles of F_j . Thus, $\mathcal{A}_j = \{F_j^{-1}(\tau_j^1), \dots, F_j^{-1}(\tau_j^q), \dots, F_j^{-1}(\tau_j^{m_j})\}$, where $\tau_j^q \in [0, 1]$ for $q = 1, \dots, m_j$. We fix each $\tau_j^1 = 0$ and $\tau_j^{m_j} = 1$, while the remaining quantiles can differ across Y_j . We require \mathcal{A}_j include $F_j^{-1}(0)$ and $F_j^{-1}(1)$. These bounds can be specified based on domain knowledge, e.g., human ages cannot be negative and are generally ≤ 110 . When an intermediate quantile is not available via external sources, it can be specified using subject-matter expertise as part of a sensitivity analysis, as described below and in Section 5.

Even though the exact map between each y_{ij} and z_{ij} is unknown, \mathcal{A}_j does provide partial information about z_{ij} under (2)–(3). We construct a set of $m_j - 1$ non-overlapping intervals that partition the support of Y_j ,

$$\mathcal{I}_j^q = (F_j^{-1}(\tau_j^q), F_j^{-1}(\tau_j^{q+1}]), \quad q = 1, \dots, m_j - 1. \quad (11)$$

Each y_{ij} belongs to exactly one \mathcal{I}_j^q . Further, $y_{ij} \in \mathcal{I}_j^q$ implies $z_{ij} \in (\Phi^{-1}(\tau_j^q), \Phi^{-1}(\tau_j^{q+1}))$ under (2)–(3); that is, if y_{ij} lies in some quantile interval, then z_{ij} must lie between the same quantiles of a standard Gaussian random variable. We visualize this mapping in Figure 1.

3.1 Estimation of the Copula Correlation

The partial mapping between y_{ij}^{obs} and z_{ij}^{obs} in Figure 1 provides the basis for estimating the copula correlation. Using the intervals in Figure 1, define the binning function

$$b_{ij}^{obs}(y_{ij}^{obs}) = q \iff y_{ij}^{obs} \in \mathcal{I}_j^q. \quad (12)$$

In what follows, we suppress the dependence of $b_{ij}^{obs}(y_{ij}^{obs})$ on y_{ij}^{obs} . Let $\mathbf{b}_i^{obs} = \{b_{ij}^{obs} : r_{ij} = 0, j = 1, \dots, p\}$ and $\mathbf{b}^{obs} = \{\mathbf{b}_i^{obs} : i = 1, \dots, n\}$. The binning in (12) has the effect of coarsening the observed data (Heitjan and Rubin, 1991; Miller and Dunson, 2018) based

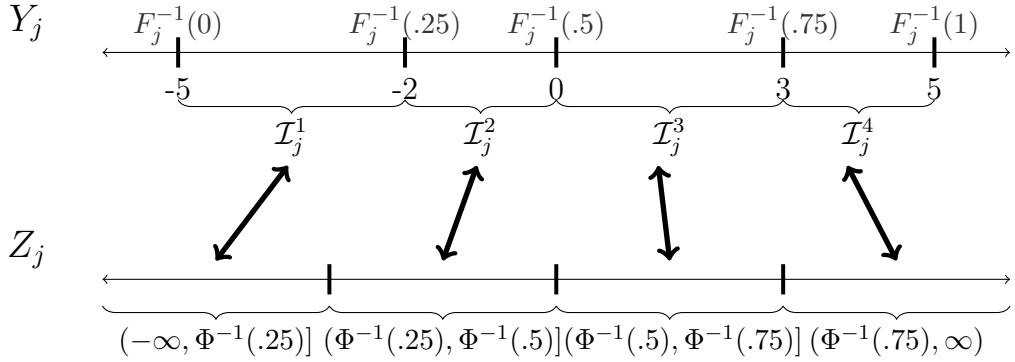


Figure 1: Using the set of auxiliary information \mathcal{A}_j to create non-overlapping intervals $\{\mathcal{I}_j^q\}_{q=1}^4$ partitioning the support of Y_j . For $y_{ij} \in \mathcal{I}_j^q$, the auxiliary quantiles defining this interval pre-determine the interval containing z_{ij} on the latent Gaussian scale. Here, $\mathcal{A}_j = \{F_j^{-1}(0) = -5, F_j^{-1}(0.25) = -2, F_j^{-1}(0.50) = 0, F_j^{-1}(0.75) = 3, F_j^{-1}(1) = 5\}$.

on the intervals defined by \mathcal{A} . Thus, we require a likelihood for $(\mathbf{C}_\theta, \boldsymbol{\alpha})$ using $(\mathbf{b}^{obs}, \mathbf{r})$.

As evident in Figure 1, whenever $b_{ij}^{obs} = q$, we must have $z_{ij}^{obs} \in (\Phi^{-1}(\tau_j^q), \Phi^{-1}(\tau_j^{q+1})]$. We represent this restriction by defining $\mathcal{D}(\mathbf{b}^{obs})$ to be the set of \mathbf{z}^{obs} satisfying the condition that each z_{ij}^{obs} is in the latent interval defined by corresponding b_{ij}^{obs} . By conditioning on \mathcal{A} rather than $\{F_j\}_{j=1}^p$, we have

$$p(\mathbf{b}^{obs}, \mathbf{r} \mid \mathbf{C}_\theta, \boldsymbol{\alpha}, \mathcal{A}) = p(\mathbf{z}^{obs} \in \mathcal{D}(\mathbf{b}^{obs}), \mathbf{z}_r \in \mathcal{E}(\mathbf{r}) \mid \mathbf{C}_\theta, \boldsymbol{\alpha}) \quad (13)$$

$$= \int \int_{\mathcal{D}(\mathbf{b}^{obs})} \int_{\mathbf{z}_r \in \mathcal{E}(\mathbf{r})} p(\mathbf{z}^{obs}, \mathbf{z}^{mis}, \mathbf{z}_r \mid \mathbf{C}_\theta, \boldsymbol{\alpha}) d\mathbf{z}_r d\mathbf{z}^{obs} d\mathbf{z}^{mis}. \quad (14)$$

The equivalence in (13) is by construction; observing \mathbf{b}^{obs} implies that \mathbf{z}^{obs} must belong to $\mathcal{D}(\mathbf{b}^{obs})$ conditional on \mathcal{A} . We refer to (13) as the extended quantile likelihood, abbreviated as EQL. The EQL also enables inclusion of discrete Y_j in the copula model, as \mathbf{b}^{obs} and \mathcal{A} can be constructed from discrete support. Extensions of the EQL to incorporate unordered categorical study variables are discussed in the supplement.

From (13), posterior inference for $(\mathbf{C}_\theta, \boldsymbol{\alpha})$ under the EQL targets

$$p(\mathbf{C}_\theta, \boldsymbol{\alpha} \mid \mathbf{z}^{obs} \in \mathcal{D}(\mathbf{b}^{obs}), \mathbf{z}_r \in \mathcal{E}(\mathbf{r}), \mathcal{A}) \propto p(\mathbf{z}^{obs} \in \mathcal{D}(\mathbf{b}^{obs}), \mathbf{z}_r \in \mathcal{E}(\mathbf{r}) \mid \mathbf{C}_\theta, \boldsymbol{\alpha}) p(\mathbf{C}_\theta, \boldsymbol{\alpha}). \quad (15)$$

We refer to the marginal posterior distribution of \mathbf{C}_θ under (15) as $\Pi_n^*(\mathbf{C}_\theta)$.

Remarkably, even when \mathcal{A} comprises only a few marginal quantiles for each study variable, it is still possible to estimate \mathbf{C}_θ accurately under the EQL in the presence of AN missingness as defined in Lemma 1, assuming of course that the full data distribution is a Gaussian copula. This fact is summarized in Theorem 2. We empirically examine the concentration of $\Pi_n^*(\mathbf{C}_\theta)$ as a function of the number of auxiliary quantiles in Section 4.1.

Theorem 2. *Suppose $\{(\mathbf{y}_i, \mathbf{r}_i)\}_{i=1}^n \stackrel{iid}{\sim} \Pi_0$ where Π_0 is the Gaussian copula with correlation \mathbf{C}_0 and marginals $\{F_j\}_{j=1}^p$ as in (2)–(3). For $j = 1, \dots, p$, suppose \mathcal{A}_j comprises $m_j \geq 3$ auxiliary quantiles of F_j , including $F_j^{-1}(0)$ and $F_j^{-1}(1)$. Let $p(\theta)$ be a prior with respect a measure that induces a prior Π over the space of all $2p \times 2p$ correlation matrices \mathbb{C} such that $\Pi(\mathbf{C}_\theta) > 0$ for all $\mathbf{C}_\theta \in \mathbb{C}$. Then, for any neighborhood \mathcal{B} of \mathbf{C}_0 , $\lim_{n \rightarrow \infty} \Pi_n^*(\mathbf{C}_\theta \in \mathcal{B}) \rightarrow 1$ almost surely $[\Pi_0]$.*

Theorem 2 provides a practically useful result when study variables have nonignorable missing values: analysts need only specify lower/upper bounds and a single intermediate quantile for each study variable to estimate \mathbf{C}_θ accurately, provided the joint distribution for (\mathbf{y}, \mathbf{r}) is a Gaussian copula and thus the missingness follows the AN mechanism of Section 2.2. Though the result is asymptotic, we demonstrate empirically in Section 4.1 that under the conditions of Theorem 2, $\Pi_n^*(\mathbf{C}_\theta)$ can concentrate rapidly with sample sizes of a few hundred. Furthermore, estimation of \mathbf{C}_θ is possible without specifying full marginal distribution models that require parameter updates for each study variable.

A similar estimation strategy for \mathbf{C}_θ is employed under the extended rank (RL) and rank-probit (RPL) likelihoods (Hoff, 2007; Feldman and Kowal, 2022), which target posterior inference for the Gaussian copula correlation by conditioning on the set of latent variables consistent with the multivariate ranks on the observed variables. However, the

Algorithm 1 Gibbs sampler for the EQL Gaussian copula

Require: prior $p(\mathbf{C}_\theta, \boldsymbol{\alpha})$, auxiliary quantiles \mathcal{A} . Let $\mathbf{C} = \mathbf{C}_\theta$.

- **Step 1:** Sample $(\mathbf{z}^{obs}, \mathbf{z}^{mis}, \mathbf{z}_r) \mid \mathbf{C}, \boldsymbol{\alpha}$

```

for  $z_{ij} \in \mathbf{z}^{obs}$  do
  Sample  $z_{ij} \sim \text{Normal}(\mu_{ij}, \sigma_j^2) \mathbb{1}(\ell_{ij}, u_{ij}]$ 
   $\ell_{ij} = \Phi^{-1}(\tau_{ij}^\ell)$ ,  $\tau_{ij}^\ell = \max\{F_j^{-1}(\tau_j^q) \in \mathcal{A}_j : y_{ij}^{obs} > F_j^{-1}(\tau_j^q)\}$ ,
   $u_{ij} = \Phi^{-1}(\tau_{ij}^u)$ ,  $\tau_{ij}^u = \min\{F_j^{-1}(\tau_j^q) \in \mathcal{A}_j : y_{ij}^{obs} \leq F_j^{-1}(\tau_j^q)\}$ 
for  $z_{ij} \in \mathbf{z}_r$  do
  Sample  $z_{ij} \sim \text{Normal}(\mu_{ij}, \sigma_j^2) \mathbb{1}(\ell_{ij}, u_{ij})$ 
   $\ell_{ij} = 0 - \infty \mathbb{1}_{r_{ij}=1}$ ,  $u_{ij} = 0 + \infty \mathbb{1}_{r_{ij}=0}$ 
for  $z_{ij} \in \mathbf{z}^{mis}$  do
  Sample  $z_{ij} \sim \text{Normal}(\mu_{ij}, \sigma_j^2)$ 
  where  $\mu_{ij} = \alpha_j + \mathbf{C}_{j(-j)} \mathbf{C}_{-(jj)}^{-1} (\mathbf{z}_{i(-j)} - \boldsymbol{\alpha}_{-j})$  and  $\sigma_j^2 = \mathbf{C}_{jj} - \mathbf{C}_{j(-j)} \mathbf{C}_{-(jj)}^{-1} \mathbf{C}_{(-j)j}$ 

```
- **Step 2:** Sample $\mathbf{C}, \boldsymbol{\alpha} \sim p(\mathbf{C}, \boldsymbol{\alpha} \mid \mathbf{z}^{obs}, \mathbf{z}^{mis}, \mathbf{z}_r)$

where $p(\mathbf{C}, \boldsymbol{\alpha} \mid \mathbf{z}^{obs}, \mathbf{z}^{mis}, \mathbf{z}_r) \propto N_{2p}((\mathbf{z}^{obs}, \mathbf{z}^{mis}, \mathbf{z}_r); \mathbf{C}, \boldsymbol{\alpha}) p(\mathbf{C}, \boldsymbol{\alpha})$

EQL and the RL/RPL make different uses of their conditioning events. Under the EQL event, \mathcal{A} partially locates \mathbf{z}^{obs} . By comparison, the RL/RPL event does not restrict where \mathbf{z}^{obs} lies in latent space, as long as the orderings of the individual z_{ij}^{obs} are consistent with the ranks of y_{ij}^{obs} . As a result, inferences for \mathbf{C}_θ under AN missingness may be biased for the RL/RPL. We demonstrate this empirically in Section 4.1.

To estimate the model, we utilize a Gibbs sampler with data augmentation (Chib and Greenberg, 1998), alternating sampling $(\mathbf{z}^{obs}, \mathbf{z}^{mis}, \mathbf{z}_r) \mid \mathbf{C}_\theta, \boldsymbol{\alpha}$ and $\mathbf{C}_\theta, \boldsymbol{\alpha} \mid (\mathbf{z}^{obs}, \mathbf{z}^{mis}, \mathbf{z}_r)$. Algorithm 1 summarizes the two steps for an arbitrary specification of $p(\mathbf{C}_\theta, \boldsymbol{\alpha})$. We present details for the $p(\mathbf{C}_\theta, \boldsymbol{\alpha})$ used in the analyses in Section 4 and the supplement. In the algorithm, the subscript $(-j)$ in a vector indicates that vector without the j th element and in the column (row) index of a matrix indicates exclusion of the elements corresponding to the j th column (row) of that matrix. The subscript $-(jj)$ in a matrix indicates exclusion of all row and column elements for the j th variable in that matrix.

Algorithm 1 offers significant computational advantages over similar samplers for RL

Gaussian copula models. Typically, $m_j << n$, so the upper and lower truncation regions in Step 1 of Algorithm 1 are shared by many observations. Consequently, the data augmentation is computationally efficient: for all $b_{ij}^{obs} = q$, corresponding z_{ij}^{obs} may be sampled simultaneously using truncated normal distributions. This enables reasonable computation times for (moderately) large n ; for example, we fit the copula model to the North Carolina data comprising nearly 170,000 children. By contrast, the computational complexity of RL Gibbs samplers depends on the number of unique marginal ranks for each Y_j , which may approach n . Because of these computational benefits, it can be advantageous to specify auxiliary quantiles for Y_j with no or MCAR missingness, for example, by letting \mathcal{A}_j for those variables comprise a set of empirical quantiles. We note that empirical quantiles may be biased if the missingness mechanism is not MCAR. For such Y_j , analysts should specify a small set of auxiliary quantiles believed to closely approximate their corresponding true quantiles and conduct sensitivity analysis to alternative specifications of \mathcal{A}_j .

3.2 Imputation with Limited Auxiliary Information

Given posterior samples of \mathbf{C}_θ and posterior predictive samples of z_{ij}^{mis} from Algorithm 1, missing study variables may be imputed through $y_{ij}^{mis} = \tilde{F}_j^{-1}(\Phi^{-1}(z_{ij}^{mis}))$, where \tilde{F}_j is an estimator of F_j . When \mathcal{A}_j contains sufficient information to outline salient features of F_j , one option is to construct \tilde{F}_j via a monotone interpolating spline through the quantiles. This expands the support of each F_j beyond the quantiles in \mathcal{A}_j . However, when \mathcal{A} comprises few quantiles, the interpolation may not accurately approximate the marginals needed for imputation. Furthermore, this strategy does not account for the uncertainty in the resulting estimate of F_j at values between the specified auxiliary quantiles. With this in mind, we describe a model-based approach for estimating intermediate quantiles of Y_j not included in \mathcal{A}_j . The method applies to any study variable, requires no modifications

of the model for \mathbf{z} , and maintains the computational benefits of the EQL.

The basic idea is to augment each \mathcal{A}_j with a finite, increasing set of s_j values, $\{y_j^q\}_{q=1}^{s_j}$, which we use as intermediate quantiles. Each y_j^q is distinct from the quantiles in \mathcal{A}_j . We specify these points to be consistent with the support of Y_j ; for example, if Y_j is discrete, each y_j^q is discrete. For Y_j taking on few values, $\{y_j^q\}$ can cover its full support. For Y_j taking on many unique values, using $s_j \approx 15$ intermediate quantiles across the range of \mathbf{y}_j^{obs} suffices to provide a discrete approximation of F_j , which we then smooth for imputation.

The key step is to coarsen \mathbf{y}^{obs} into bins using both the quantiles in \mathcal{A} and intermediate quantiles in $\{y_j^q\}_{q=1}^{s_j}$, through which we can relate the latent variables to the binned data. In doing so, we maintain the ordering between auxiliary and intermediate quantiles on the latent scale. Let $\mathcal{A}_j^* = \mathcal{A}_j \cup \{y_j^q\}_{q=1}^{s_j}$, $a_j = |\mathcal{A}_j^*|$, and $\mathcal{A}^* = \{\mathcal{A}_j^*\}_{j=1}^p$. Using \mathcal{A}_j^* , we construct $a_j - 1$ disjoint intervals $\{\mathcal{I}_j^1, \dots, \mathcal{I}_j^{a_j}\}$ like those in (11), partitioning the support of Y_j at the a_j points in \mathcal{A}_j^* . We then define b_{ij}^{obs} similarly to (12) but based on the $a_j - 1$ intervals. The interval for z_{ij}^{obs} is determined relative to the closest auxiliary quantiles in \mathcal{A}_j and adjacent intermediate points in $\{y_j^q\}$. This is illustrated in Figure 2. Using the mapping from the intervals to the latent variables allows us to estimate \mathbf{C}_θ and $F_j(y_j^q)$.

We first formally describe the method, followed by motivation for why it works. Whenever $b_{ij}^{obs} = q$ (and analogously, $y_{ij}^{obs} \in \mathcal{I}_j^q$) we have $\ell_{ij} < z_{ij}^{obs} < u_{ij}$, where

$$\ell_{ij} = \max\{\Phi^{-1}(\tau_{ij}^\ell), \max(z_{vj}^{obs} : b_{vj} = q - 1); v = 1, \dots, n\} \quad (16)$$

$$u_{ij} = \min\{\Phi^{-1}(\tau_{ij}^u), \min(z_{vj}^{obs} : b_{vj} = q + 1); v = 1, \dots, n\}$$

and $\tau_{ij}^\ell, \tau_{ij}^u$ are defined as in Step 1 of Algorithm 1. The interval (ℓ_{ij}, u_{ij}) ensures that whenever $b_{ij}^{obs} < b_{vj}^{obs}$ we have $z_{ij}^{obs} < z_{vj}^{obs}, i \neq v$. With intermediate points determined analogously for (Y_1, \dots, Y_p) , we define the quantile ordering set restriction $\mathcal{D}^*(\mathbf{b}^{obs})$, which incorporates the intermediate quantiles to encode the condition that z_{ij}^{obs} is in the interval

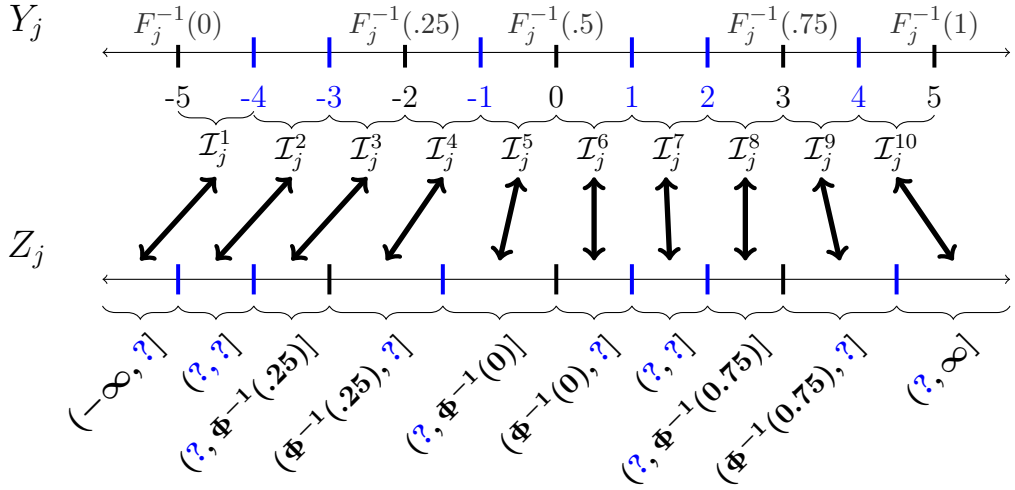


Figure 2: Augmenting \mathcal{A}_j with intermediate points $\{y_j^q\} = \{-4, -3, -1, 1, 2, 4\}$. Thus, $|\mathcal{A}_j^*| = 11$. For $y_{ij} \in \mathcal{I}_j^q$ with at least one intermediate endpoint, the unknown bounds on the latent interval containing z_{ij} are represented by the question marks.

(16) corresponding to its b_{ij}^{obs} . We replace \mathcal{A} with \mathcal{A}^* and $\mathcal{D}(\mathbf{b}^{obs})$ with $\mathcal{D}^*(\mathbf{b}^{obs})$ in (13) and (14) to estimate \mathbf{C}_θ . We refer to this variation as the extended hybrid quantile likelihood (EHQL). Estimating the copula correlation under the EHQL requires minor modifications to Algorithm 1, namely replacing the truncation bounds for z_{ij}^{obs} in Step 1 with (16).

The modified Algorithm 1 produces draws of each z_{ij}^{obs} . For any interval \mathcal{I}_j^q constructed using an intermediate point as an upper bound, define $Z_j^q = \max\{z_{ij}^{obs} : b_{ij}^{obs} = q\}$. With enough observations having $b_{ij}^{obs} = q$, Algorithm 1 should generate values of z_{ij}^{obs} that cover much of the interval on the latent scale corresponding to \mathcal{I}_j^q . When this is the case, we should sample a Z_j^q that is close to the corresponding $\Phi^{-1}(F_j(y_j^q))$ under the copula model. Using each sampled Z_j^q from Algorithm 1, for all j and q , we compute posterior draws of

$$\tilde{F}_j(y_j^q) = \Phi(Z_j^q). \quad (17)$$

The draws of (17) provide estimates of uncertainty about the intermediate quantiles. When few individuals have $b_{ij}^{obs} = q$, which may occur for intervals constructed at quantiles in the tails, we expect higher uncertainty in the draws of $\tilde{F}_j(y_j^q)$. This is borne out in the

Algorithm 2 Estimating F_j under the EHQL Gaussian copula

Require: \mathcal{A}^* and one draw of \mathbf{z}^{obs} from Algorithm 1
Return: One draw $\{\tilde{F}_j(y_j^q)\}_{q=1}^{s_j}$, $j \in \{1, \dots, p\}$
for $j \in \{1, \dots, p\}$ **do**
 Compute $Z_j^q = \max\{z_{ij}^{obs} : b_{ij}^{obs} = q\}$ for each element in $\{y_j^q\}_{q=1}^{s_j}$
 Compute $\tilde{F}_j(y_j^q) = \Phi(Z_j^q)$

simulations of Section 4. Algorithm 2 summarizes the process of estimating $\{\tilde{F}_j(y_j^q)\}$.

For imputation, we interpolate between posterior samples of $\{y_j^q, \tilde{F}_j(y_j^q)\}_{q=1}^{s_j}$ and the points in \mathcal{A}_j via a monotone spline, fit using the package `splinefun` in R. Because the upper and lower bounds of \mathcal{A}_j^* are fixed, the smoothing step is guaranteed to produce samples of a valid distribution function that pass through the points in \mathcal{A}_j^* . We use these versions of \tilde{F}_j to impute each y_{ij}^{mis} at any iteration of Algorithm 1 by setting $y_{ij}^{mis} = \tilde{F}_j^{-1}(\Phi(z_{ij}^{mis}))$.

Using (17) in addition to \mathcal{A}_j to approximate F_j has advantages over approximating F_j based on the quantiles in \mathcal{A}_j alone, as done in the EQL. First, $\{y_j^q\}$ lends more information to the discrete approximation, helping the estimator better capture features of each marginal. Second, the draws of $\Phi(Z_j^q)$ in (17) propagate uncertainty about $F_j(y_j^q)$ to the imputations, whereas the EQL interpolation of $F_j(y_j^q)$ is deterministic. For these reasons, we recommend employing the EHQL for copula estimation and Algorithm 2 for marginal CDF estimation whenever imputation is needed. We note that Feldman and Kowal (2024) used a strategy similar to (17) for the RL Gaussian mixture copula under MAR mechanisms.

4 Simulation Studies

In this section, we present results of simulation studies evaluating (i) the impact of the level of detail in the marginal distributions on the quality of inferences and (ii) the repeated sampling performance of the model as a multiple imputation engine compared to alternative methods that do not use the auxiliary information for imputations.

In the simulations as well as the analysis of the North Carolina data in Section 5, the

prior distribution on the parameters $\boldsymbol{\theta}$ that index $\mathbf{C}_{\boldsymbol{\theta}}$ is the factor model,

$$\mathbf{z}_i = \boldsymbol{\alpha} + \boldsymbol{\Lambda} \boldsymbol{\eta}_i + \boldsymbol{\epsilon}_i, \quad \boldsymbol{\epsilon}_i \sim N_{2p}(\mathbf{0}, \boldsymbol{\Sigma}). \quad (18)$$

Here, $\boldsymbol{\Lambda}$ is a $(2p) \times k$ matrix of factor loadings possibly with $k << 2p$; $\boldsymbol{\eta}_i$ is a $k \times 1$ vector of factors; and, $\boldsymbol{\Sigma} = \text{diag}(\sigma_1^2, \dots, \sigma_{2p}^2)$. By specifying $\boldsymbol{\eta}_i \sim N_k(\mathbf{0}, \mathbf{I}_k)$, where \mathbf{I}_k is the $k \times k$ identity matrix, marginally we have $\mathbf{z}_i \sim N_{2p}(\boldsymbol{\alpha}, \boldsymbol{\Omega})$, where $\boldsymbol{\Omega} = \boldsymbol{\Lambda} \boldsymbol{\Lambda}^\top + \boldsymbol{\Sigma}$ is the reduced rank covariance. Thus, $\boldsymbol{\theta} = (\boldsymbol{\Lambda}, \boldsymbol{\Sigma})$. Given posterior samples of $\boldsymbol{\Omega}$, samples of $\mathbf{C}_{\boldsymbol{\theta}}$ are obtained by scaling $\boldsymbol{\Omega}$ into correlations. The prior on the factor loadings provides shrinkage, automating rank selection (Bhattacharya and Dunson, 2011). In addition, the components of \mathbf{z}_i are independent conditional on $\boldsymbol{\eta}_i$, which benefits computation, especially in Step 1 of Algorithm 1. The full hierarchical specification of (18) is available in the supplement.

4.1 Accuracy with Sparse Auxiliary Information

Theorem 2 provides posterior consistency for the copula correlation when each \mathcal{A}_j comprises at least $m_j \geq 3$ ground truth quantiles. In this section, we investigate how sensitive the contraction of the posterior is to the cardinality of \mathcal{A}_j .

We simulate $2p$ -dimensional observations $\{(\mathbf{y}_i, \mathbf{r}_i)\}_{i=1}^n$ for $n \in \{200, 1000, 5000\}$ and $p \in \{5, 10, 20\}$ from Gaussian copulas. For each (n, p) , we randomly generate \mathbf{C}_0 from a scaled inverse-Wishart distribution. Since each entry of \mathbf{C}_0 is non-zero, this generates nonignorable missingness per Lemma 1. We vary the amount of missing data by setting $\Phi(\alpha_{r_j}) \in \{0.25, 0.50\}$. Thus, marginally, missingness in each study variable is approximately 25% or 50%. For $j \leq p$, we vary F_j so that $Y_j \sim \text{Gamma}(1, 1)$ when $j \in \{1, 4, 7, \dots\}$; $Y_j \sim \text{t}(\nu = 5, ncp = 2)$ when $j \in \{2, 5, 8, \dots\}$; and, $Y_j \sim \text{Beta}(1, 2)$ when $j \in \{3, 6, 9, \dots\}$. Here, ν and ncp are a degrees of freedom and non-centrality parameter. Each z_{ij} for $j \leq p$ is transformed to y_{ij} via $F_j^{-1}(\Phi(\tilde{z}_{ij}))$. When $z_{i(p+j)} > 0$, we set $r_{ij} = 1$ and make y_{ij} missing.

We estimate the copula using Algorithm 1, incorporating three granularities of \mathcal{A} .

The first includes the fully specified, true $\{F_j\}_{j=1}^p$, referred to as “Full.” The second is significantly more sparse, using just the lower/upper bounds and median, i.e., each $\mathcal{A}_j = \{F_j^{-1}(0), F_j^{-1}(0.5), F_j^{-1}(1)\}$. This is referred to as “EQL-M.” The supplement includes results for variants of EQL where \mathcal{A} comprises deciles and every fourth quantile.

We also employ the EHQL, with each $\mathcal{A}_j = \{F_j^{-1}(0), F_j^{-1}(0.5), F_j^{-1}(1)\}_{j=1}^p$ and $s_j \approx 15$ intermediate quantiles. We refer to this as “EHQL-M.” The intermediate quantiles are constructed in each simulation run by first specifying 20 evenly spaced bins over the range of \mathbf{y}_j^{obs} and creating $\{\mathcal{I}_j^q\}$ based on the bins occupied by the observed data. This results in approximately 15 intermediate points in each simulation run.

We generate several datasets for each $(n, p, \boldsymbol{\alpha})$ setting. For each dataset and \mathcal{A} , we simulate 1000 posterior samples of \mathbf{C}_θ . We emphasize that fitting EQL-M and EHQL-M in these datasets does not simply parrot the data generating model, as they use only a sparse set of marginal quantiles in \mathcal{A} . We also include comparisons to the copula fit under the RL of Hoff (2007), which we estimate using the `sbgcop` package in R. Although the RL copula is a joint model for (\mathbf{y}, \mathbf{r}) , it does not leverage any information beyond the observed data.

Let $\rho_{\theta,uv}$ represent the element (correlation) in row u and column v of \mathbf{C}_θ . Similarly, let $\rho_{0,uv}$ be the corresponding element in the \mathbf{C}_0 used in data generation. Figure 3 displays 95% credible intervals based on 1000 draws of $\rho_{0,uv} - \rho_{\theta,uv}$ for the $2p(2p-1)/2$ unique correlation coefficients for one randomly selected dataset in the $p = 5$ and 50% missingness scenario. Results for other datasets and settings are qualitatively similar; see the supplement.

Theorem 2 implies that, under the EQL, $\rho_{0,uv} - \rho_{\theta,uv}$ should converge to 0 as sample size increases. This is confirmed in Figure 3 for all versions of \mathcal{A} . The credible intervals under EQL-M are slightly wider than those under Full, which suggests a loss in efficiency with lower levels of auxiliary information. The intervals for EHQL-M are virtually indis-

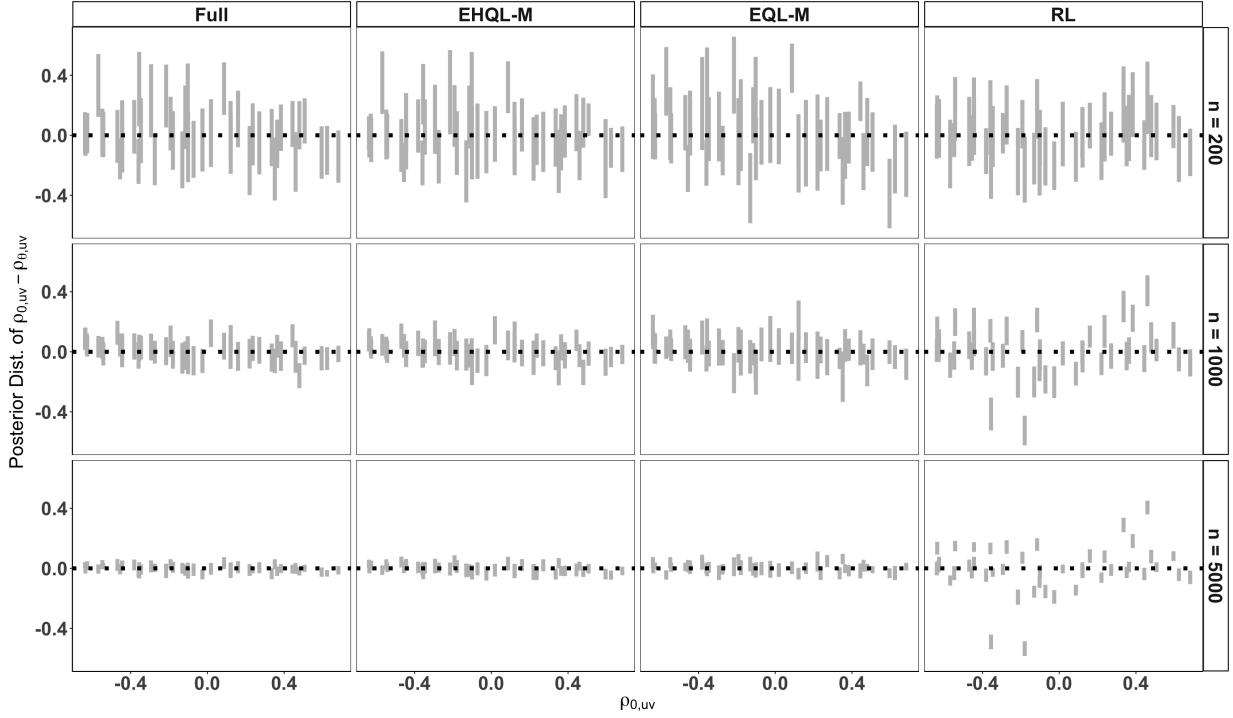


Figure 3: Plots of 95% credible intervals for $\rho_{0,uv} - \rho_{\theta,uv}$ for all unique correlations in \mathbf{C}_0 using various \mathcal{A} for three sample sizes. “Full” uses full marginals; “EQL-M” uses the lower/upper bounds and median; “EHQL-M” augments each \mathcal{A}_j for EQL-M with $s_j \approx 15$ estimated intermediate quantiles. Results are presented for scenario with 50% missing values for each of $p = 5$ study variables. The right-most column provides results for the copula correlation estimated under the RL. For the larger sample sizes, posterior inference for \mathbf{C}_θ under the EQL/EHQL is accurate with minor efficiency losses when incorporating fewer auxiliary quantiles. In contrast, the inferences under RL can be biased.

tinguishable from those for Full. Even though EHQL-M and EQL-M leverage the same \mathcal{A} , EHQL-M makes greater use of the information in \mathbf{y}^{obs} by better locating the corresponding \mathbf{z}^{obs} , which improves precision. By contrast, for the two larger values of n , estimates of \mathbf{C}_θ under the RL copula are significantly biased. Finally, for $n = 200$, the sampling variability is sufficiently large that inferences for all four methods are not obviously different qualitatively.

We run each EQL/EHQL and RL sampler for 10,000 iterations on a 2023 Macbook Pro. When $n = 5000$, the EQL/EHQL samplers average around five minutes to complete, whereas the RL sampler takes nearly four hours. Mixing is also facilitated by introducing

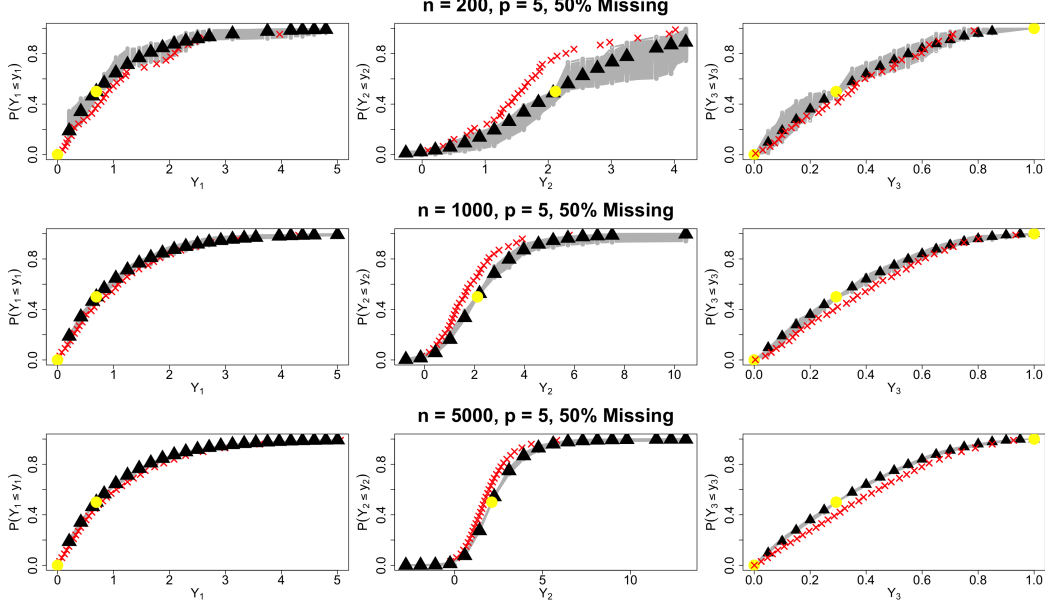


Figure 4: EHQL posterior samples of \tilde{F}_j (lines) compared to true $F_j(y_j^q)$ (triangles) and empirical CDFs (crosses) computed from \mathbf{y}^{obs} . Columns index $j = 1, 2, 3$ from left to right. Rows index the sample size. Each \mathcal{A}^* uses the lower/upper bounds and the median (dots) and 15 intermediate quantiles. The proposed estimator accurately outlines each true CDF and corrects the biases in the ECDF caused by nonignorable missingness.

\mathcal{A} , with apparent convergence of the posterior of \mathbf{C}_θ after a few hundred samples.

Finally, we evaluate how closely (17) under the EHQL-M approximates each true F_j .

Figure 4 displays posterior samples of $\tilde{F}_j(y_j^q)$ for $j = 1, 2, 3$ evaluated at the specified intermediate quantile points; it also displays the empirical CDFs (ECDF) computed from \mathbf{y}^{obs} . These ECDFs exhibit varying degrees of bias caused by the nonignorable missing data. In contrast, each $\tilde{F}_j(y_j^q)$ accurately approximates the general shape of F_j , even though \mathcal{A} only includes bounds and medians. As expected, posterior uncertainty with (17) is highest for regions with relatively small sample sizes.

4.2 Simulation of Repeated Sampling Performance

In this simulation study, we evaluate repeated sampling properties of the EHQL copula with multiple imputation inferences. We use $p = 5$ variables from the North Carolina lead exposure data displayed in Table 5, namely Economically Disadvantaged (EconDisadv),

Mother's Age (`mAge`), Mother's Race (`mRace`), an index of Neighborhood Deprivation (`NDI`), and end-of-fourth grade (EoG) standardized math test scores (`Math_Score`). These variables are mixed binary, unordered categorical, count, and continuous variables that have complex univariate and multivariate features. We collect all individuals with complete data on these five variables, excluding observations with $|\text{NDI}| > 5$ to provide stability, which we treat as a finite population comprising approximately 165,000 individuals. Using this population, we estimate 10th, 50th, and 90th quantile regressions (Koenker, 2010) of `Math_Score` on main effects of the other four variables, which we treat as population quantities. The target models aim to uncover potentially heterogeneous effects of the covariates depending on the level of academic achievement, previewing the analysis in Section 5.

We take 500 simple random samples of $n = 5000$ individuals from this constructed population. In each sample, we generate nonignorable missingness in `NDI`. Letting $j = 1$ index the variable corresponding to `NDI`, we do so by the missingness mechanism,

$$p(R_{i1} = 1 \mid \mathbf{y}) \sim \text{Bernoulli}(\Phi(-0.5 - 1.3y_{i1}^{scale})), \quad (19)$$

where superscript *scale* indicates that the variable is centered and scaled to unit variance. After deleting any y_{i1} where $r_{i1} = 1$, we have approximately 40% missing values of `NDI`, with lower values more likely to be missing in the sampled data. We also randomly remove 5% of the other variables, including `Math_Score`. Because of the nonignorable missingness, complete case analysis could result in biased estimates of the quantile regression coefficients.

As auxiliary information, we assume access to selected quantiles of `NDI`, which we take from its marginal distribution in the constructed population. Here, we let \mathcal{A} include the lower/upper bounds and median. The supplement includes results using the lower/upper bounds and 75th quantile, which are qualitatively identical to those presented here. We implement the EHQL using 15 evenly spaced quantiles across the range of observed values

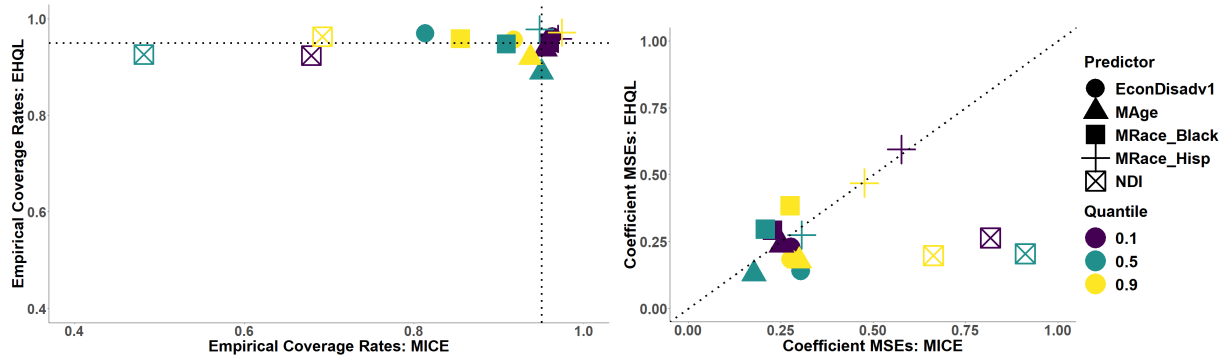


Figure 5: Empirical coverage rates (left) and mean squared error (MSE) of multiple imputation point estimates (right) for the EHQL copula and MICE imputations in the repeated simulation study. For the coefficients of NDI, the EHQL provides significantly lower bias and higher coverage rates. While not shown, the average interval widths are similar.

of NDI. For the other study variables, we use the empirical deciles in the sampled data as the quantiles in \mathcal{A} . We add a missingness indicator for NDI to the Gaussian copula model. We exclude the remaining indicators, which effectively models that data for the corresponding variables are MCAR.

We run the Gibbs sampler in Algorithm 1 for 5,000 iterations. After a conservative burn-in of 2,500 draws, we extract interpolated CDFs for imputation using Algorithm 2, and take the completed data in every 125th iteration to create $m = 20$ multiple imputations. We estimate the targeted quantile regressions and use the combining rules of Rubin (1987) for point estimates and 95% confidence intervals for the quantile regression coefficients. We also implement a default application of multiple imputation by chained equations (MICE) based on the `mice` package in R (van Buuren, 2018). This does not use \mathcal{A} , although we add R_1 as a predictor for MICE. We repeat the entire procedure of sampling 5000 individuals, making missing values, and obtaining multiple imputation inferences 500 times.

Figure 5 summarizes the multiple imputation inferences over the 500 runs. The inferences for the coefficients subject to MCAR missingness are reasonably similar for EHQL and MICE, and generally of high quality. However, we see substantial differences among EHQL

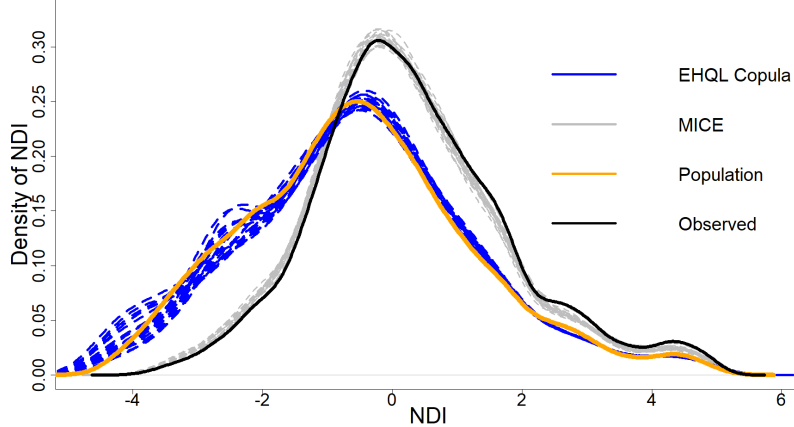


Figure 6: Marginal distribution of NDI in 20 completed datasets produced by EHQL and MICE. The EHQL imputations capture the bi-modality and skewness of the population marginal, whereas the MICE imputations mimic the distribution of the observed values.

and MICE coefficient estimates for NDI. These coefficients are accurately estimated with close to nominal coverage rates under EHQL, but not MICE. Evidently, the incorporation of \mathcal{A} and the flexible dependence structure under the copula model allow the imputations to reflect the multivariate relationships more accurately than MICE does. The advantage of EHQL relative to MICE is also evident in the imputations of NDI, which match the population marginal for EHQL but do not for MICE. This is visualized in Figure 6.

5 Analysis of North Carolina Lead Exposure Data

Public health research in recent years has concluded overwhelmingly that lead exposure has adverse impacts on childhood cognitive development (e.g., [Bellinger et al., 1992](#); [Miranda et al., 2009](#); [Kowal et al., 2021](#); [Bravo et al., 2022](#)). Many studies investigating this topic rely on administrative health and education datasets, linked at the individual child level, to estimate associations between lead exposure and outcomes of interest. Typically, blood-lead measurements are available only for children who are tested for lead exposure, and children are more likely to be tested when there is concern about their exposure ([Kamai et al., 2022](#)). Consequently, abundant missingness among lead measurements is common-

Variable Name	$\bar{Y}^{obs}/\bar{Y}^{mis}$	Description
Blood_lead	2.79/NA	Blood lead level (micrograms per deciliter)
Math_Score	448.9/452.5	Standardized score on first 4th grade EoG math test
Reading_Score	445.2/448.5	Standardized score on first 4th grade EoG reading test
mEduc	(.25, .56, .21)/ (.10, .48, .42)	Mother's education at the time of birth (No degree, High school degree, College degree)
mRace	(.57,.31,.12)/ (.76,.19,.05)	Mother's race/ethnicity (Non-Hispanic (NH) White, NH Black, Hispanic)
BWTpct	46.9/51.7	Birthweight percentile
mAge	25.9/28.7	Mother's age at the time of birth
Gestation	38.6/38.7	Gestational period (in weeks)
Male	.50/.50	Male infant (1 = Yes, 0 = No)
Smoker	.15/.09	Mother smoked (1 = Yes, 0 = No)
NotMarried	.46/.22	Not married at time of birth (1 = Yes, 0 = No)
EconDisadv	.61/.32	Economically disadvantaged, per participation in the Child Nutrition Lunch Program (1 = Yes, 0 = No)
RI	.23/.18	Residential isolation index, at time of EoG test
NDI	.10/-1.04	Neighborhood Deprivation Index, at time of EoG test

Table 1: Variables used in the analysis of the relationship between lead exposure and EoG test scores among fourth grade children in North Carolina. Data are restricted to children with 30–42 weeks of gestation, 0–104 weeks of age-within-cohort, mother's age 15–44, $\text{Blood_Lead} \leq 10$, birth order ≤ 4 , no status as an English Language Learner, and residence in North Carolina at the time of birth and the time of the EoG test. For the quantile regressions, numeric covariates are scaled to mean 0 with 0.5 standard deviation.

place, and individuals who are measured tend to have higher levels of exposure than much of the population. Accurate imputation of lead measurements is important in this setting, as selection biases could influence population-level inferences on the associations between cognitive outcomes and lead exposure (e.g., as simulated in Section 4.2).

We analyze a dataset containing information on $\sim 170,000$ North Carolina children born between 2003 and 2005. The dataset is constructed by linking children's data across three databases comprising (i) detailed birth records, which include maternal demographics, maternal and infant health measures, and maternal obstetrics history for all documented live births in N.C.; (ii) lead exposure surveillance records from a registry maintained by the state of N.C., which include integer-valued blood-lead levels; and (iii) test score data from the N.C. Education Research Data Center at Duke University, which include EoG reading

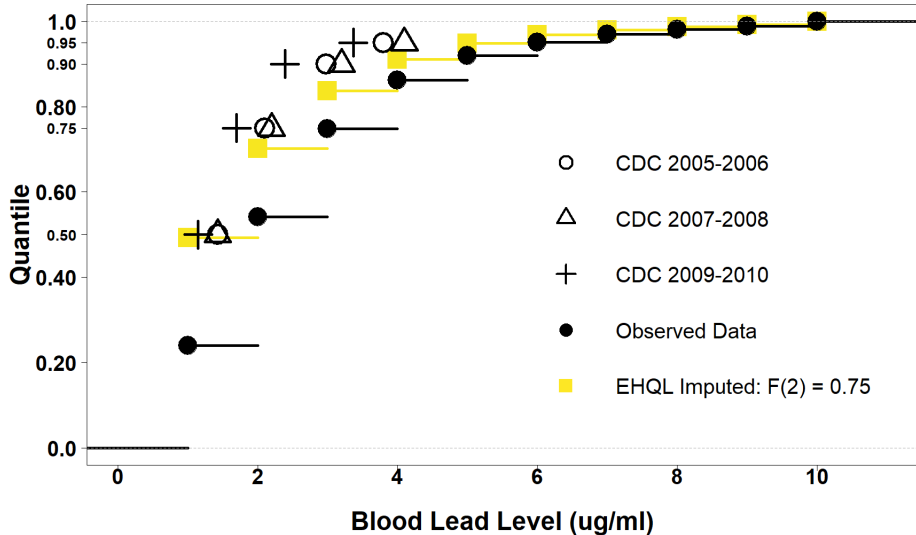


Figure 7: Empirical distribution of `Blood_lead` in the North Carolina data and population-level quantiles published by the CDC. Also displayed are average estimated quantiles of `Blood_lead` in completed datasets after EHQL imputations. We include CDC values consistent with the years most children were measured for lead exposure. After imputation, the marginal distribution of `Blood_lead` more closely matches the population-level estimates.

and mathematics test scores as well as some demographic and socioeconomic information (CEHI, 2020). Table 1 summarizes the variables we use, including their sample averages among children with lead exposure (`Blood_lead`) observed or missing. Notably, 35% of the lead measurements are missing. Other variables have missing data rates less than 0.02%.

Figure 7 displays the ECDF of `Blood_lead` compared to three years of annual point estimates for the 50th, 75th, 90th, and 95th quantiles of lead exposure levels published by the CDC (Centers for Disease Control and Prevention, 2022). Clearly, the observed distribution does not match the population-level quantile estimates. We therefore consider the missingness in `Blood_lead` as possibly missing not at random (MNAR). As we discuss later, the EHQL copula correlation estimates suggest this missingness in fact is MNAR.

To adjust for this missingness, we seek to leverage the CDC estimates as auxiliary information for `Blood_lead`. However, the `Blood_lead` measurements in the North Carolina data are recorded as integers corresponding to the interval in which the child's measurement

is contained. For instance, `Blood_lead=1` means that the child's measurement was in the interval $(0, 1] \mu\text{g}/\text{ml}$. By contrast, the CDC measurements are continuous. In addition, the CDC estimates are national, which ignores regional or state-specific effects.

We therefore use the CDC estimates to approximately locate the marginal distribution of `Blood_lead` and employ Algorithm 2 to infer intermediate quantiles. As evident in Figure 7, the 75th quantile estimates from the three years of CDC publications are reliably around 2.0. Because of this stability, we set $\mathcal{A}_{\text{Blood_lead}} = \{F_{\text{Blood_lead}}^{-1}(0) = 0, F_{\text{Blood_lead}}^{-1}(0.75) = 2, F_{\text{Blood_lead}}^{-1}(1) = 10\}$. We also examine sensitivity of results when using $F_{\text{Blood_lead}}^{-1}(0.70) = 2$ and $F_{\text{Blood_lead}}^{-1}(0.80) = 2$. For the remaining numerical study variables, we use empirical deciles for the auxiliary quantiles. This is reasonable given the scarce missingness and large sample size. These auxiliary quantiles are not varied in the sensitivity analysis.

We use the EHQL copula with the factor model in (18) to implement multiple imputation of all missing values. We include a missingness indicator for `Blood_lead` but not the other variables, which are almost completely observed. Their indicators comprise almost all zeros and thus are not likely to inform the imputation but would slow computation. Consequently, the remaining study variables are treated as MCAR. For each set of auxiliary information, we estimate the EHQL copula by running Algorithm 1 for 10,000 iterations and discarding 5,000 draws as burn-in. We use every 250th posterior sample of model parameters to create $m = 20$ multiple imputations. Posterior predictive checks suggest that the model reasonably describes the observed data; these are available in the supplement.

Using the completed datasets, we estimate the 10th, 50th, and 90th quantile regressions of math and reading scores on main effects of all the study variables, and derive point estimates and uncertainty quantification using multiple imputation combining rules. These quantities describe potentially heterogeneous impacts of the covariates on low, middle, and

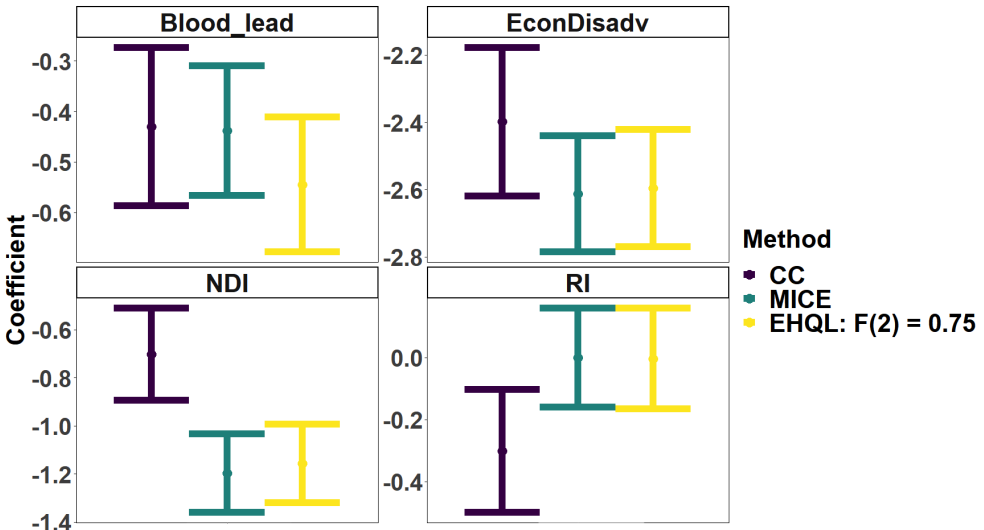


Figure 8: Multiple imputation inferences for coefficients of 10th quantile regression when `Blood_lead` = 2 is the 75th quantile of the marginal distribution. Compared to complete case analysis, we see sizeable differences especially for the coefficient of `Blood_lead`. It is estimated to be more adversely associated with EoG math scores. MICE imputations do not capture this difference for `Blood_lead`, as MICE mimics patterns in the observed data.

high-achieving students, which is of interest to public health research ([Miranda et al., 2009](#)).

Figure 8 summarizes the multiple imputation inferences for the 10th quantile regression coefficients for `Blood_lead`, `EconDisadv`, `NDI`, and `RI` using `Math_Score` as the response. The results are presented for $F_{\text{Blood_lead}}^{-1}(0.75) = 2$; the findings are insensitive to the other values of this auxiliary quantile. We compare these inferences to those obtained by fitting the quantile regression models to complete case (CC) observations, which exclude any observations with missing study variables, and to results from $m = 20$ multiple imputations using a bespoke application of MICE. Results for the other auxiliary quantile specifications, quantile regressions, and using reading scores as the response are in the supplement.

After multiple imputation, we see sizeable shifts in the inferences. The estimated associations of `Blood_lead`, `EconDisadv`, and `NDI` with `Math_Score` are more adverse than in the CC analysis. The association of `Blood_lead` with `Math_Score` is estimated to be significantly stronger when using the EHQL imputations rather than the MICE imputations.

Specifically, the point estimate for this coefficient under the EHQL is nearly two standard errors more negative than point estimates under CC and MICE, which is a substantively large change. The inferences under EHQL and MICE are similar for the other predictors' coefficients, which is not unexpected as these variables have few missing values. Similar shifts are evident in the 50th and 90th quantile regressions as well.

To illuminate the effect of the EHQL imputations further, we examine the empirical CDF of `Blood_lead` obtained by averaging across the 20 completed datasets; this is displayed in Figure 7. Because it utilizes \mathcal{A} , the EHQL imputes values of missing `Blood_lead` measurements that are small relative to the observed values. Simultaneously, the percentiles of EoG math scores are higher for students missing `Blood_lead` than for students with recorded values. Consequently, imputing `Blood_lead` so that its completed-data distribution accords with \mathcal{A} strengthens its negative association with `Math_Score`. We see similar strengthening of inverse associations with the other predictors except for `RI`, which has estimates mostly shrunk towards zero. `RI` is strongly correlated to `NDI`, which may help explain why its estimates attenuate. We note that a 95% credible interval for the copula correlation between `Blood_lead` and its missingness indicator is $(-0.92, -0.91)$, offering additional evidence that the missingness in lead exposure measurements is MNAR.

6 Concluding Remarks

Using auxiliary marginal quantiles offers a convenient and flexible way to handle nonignorable missing data in Gaussian copula models. The simulation studies suggest that using reliable \mathcal{A} —for example, informed by external sources like national surveys or administrative databases—can result in more accurate inferences than treating nonignorable missing data as MCAR or MAR. In fact, under AN missingness, it is possible to estimate accurately the copula correlation and perform well-calibrated multiple imputation even with just a few

auxiliary quantiles on each study variable. The simulations also suggest that augmenting \mathcal{A} with intermediate quantiles can improve the quality of inferences and imputations.

There are many topics worthy of future research. For example, the marginal quantiles may be known with uncertainty, for example, estimates from a probability sample. In cases where analysts desire a single inference, it may be possible to posit sampling distributions for the true quantiles that can be integrated into the model specification. Additionally, often data have survey weights. While there are methods for using auxiliary margins with survey-weighted data for categorical data models (Akande and Reiter, 2022; Tang et al., 2024), work is needed to develop methods for the EQL/EHQL copulas.

The North Carolina lead exposure analysis suggests that utilizing auxiliary marginal quantiles to handle nonignorable missing data can impact empirical findings. In particular, inferences drawn from the multiple imputations based on the EHQL copula suggest that lead exposure affects childhood cognitive development more adversely than might be concluded from a complete case analysis. More broadly, linked data like these are commonly used in public health studies and full of missing values. When the missingness may be MNAR, analysts can consider imputation strategies that leverage known marginal quantiles of the study variables to better inform health policy and intervention strategies.

References

Akande, O., Madson, G., Hillygus, D. S., and Reiter, J. P. (2021). Leveraging auxiliary information on marginal distributions in nonignorable models for item and unit nonresponse. *Journal of the Royal Statistical Society Series A*, 184:643–662.

Akande, O. and Reiter, J. P. (2022). Multiple imputations for nonignorable item nonresponse in complex surveys using auxiliary margins. In *Statistics in the Public Interest: In Memory of Stephen E. Fienberg*, pages 289–306. Cham: Springer.

Bellinger, D. C., Stiles, K. M., and Needleman, H. L. (1992). Low-level lead exposure, intelligence and academic achievement: a long-term follow-up study. *Pediatrics*, 90:855–861.

Bhattacharya, A. and Dunson, D. B. (2011). Sparse Bayesian infinite factor models. *Biometrika*, 98:291–306.

Bravo, M. A., Zephyr, D., Kowal, D., Ensor, K., and Miranda, M. L. (2022). Racial residential segregation shapes the relationship between early childhood lead exposure and fourth-grade standardized test scores. *Proceedings of the National Academy of Sciences*, 119:e2117868119.

CEHI (2020). Linked births, lead surveillance, grade 4 end-of-grade scores [data set].

Centers for Disease Control and Prevention (2022). CDC Exposure Report Data Tables. https://www.cdc.gov/exposurereport/data_tables.html.

Chib, S. and Greenberg, E. (1998). Analysis of multivariate probit models. *Biometrika*, 85:347–361.

Chiba, D., Martin, L. W., and Stevenson, R. T. (2015). A copula approach to the problem of selection bias in models of government survival. *Political Analysis*, 23:42–58.

Christoffersen, B., Genz, A., Bretz, F., and Hothorn, T. (2023). mdgc: Missing data imputation using Gaussian copulas. R package version 0.1.7.

Deng, Y., Hillygus, D. S., Reiter, J. P., Si, Y., and Zheng, S. (2013). Handling attrition in longitudinal studies: The case for refreshment samples. *Statistical Science*, 28:238–256.

Di Lascio, F., Giannerini, S., and Reale, A. (2015). Exploring copulas for the imputation of complex dependent data. *Statistical Methods and Application*, 24:159–175.

Eckert, C. and Hohberger, J. (2023). Addressing endogeneity without instrumental variables: An evaluation of the Gaussian copula approach for management research. *Journal of Management*, 49:1460–1495.

Fan, Y. and Patton, A. J. (2014). Copulas in econometrics. *Annual Review of Economics*, 6:179–200.

Feldman, J. and Kowal, D. R. (2022). Bayesian data synthesis and the utility-risk trade-off for mixed epidemiological data. *The Annals of Applied Statistics*, 16:2577–2602.

Feldman, J. and Kowal, D. R. (2024). Nonparametric copula models for multivariate, mixed, and missing data. *Journal of Machine Learning Research*, 25(164):1–50.

Heitjan, D. F. and Rubin, D. B. (1991). Ignorability and coarse data. *The Annals of Statistics*, 49:2244–2253.

Hirano, K., Imbens, G. W., Ridder, G., and Rubin, D. B. (2001). Combining panel data sets with attrition and refreshment samples. *Econometrica*, 69:1645–1659.

Hoff, P. D. (2007). Extending the rank likelihood for semiparametric copula estimation. *The Annals of Applied Statistics*, 1:265–283.

Hoff, P. D. (2022). sbgcop: Semiparametric Bayesian Gaussian copula estimation and imputation. R package version 0.980.

Hollenbach, F. M., Bojinov, I., Minhas, S., Metternich, N. W., Ward, M. D., and Volfovsky, A. (2021). Multiple imputation using Gaussian copulas. *Sociological Methods & Research*, 50:1259–1283.

Joe, H. (2014). *Dependence Modeling with Copulas*. Chapman & Hall/CRC Press.

Käärik, M. and Käärik, E. (2010). Imputation by Gaussian copula model with an application to incomplete customer satisfaction data. In Lechevallier, Y. and Saporta, G., editors, *Proceedings of COMPSTAT'2010*, pages 485–492. Physica-Verlag HD.

Kamai, E. M., Daniels, J. L., Delamater, P. L., Lanphear, B. P., MacDonald Gibson, J., and Richardson, D. B. (2022). Patterns of children’s blood lead screening and blood lead levels in North Carolina, 2011–2018 — who is tested, who is missed? *Environmental Health Perspectives*, 130:067002.

Koenker, R. (2010). *Quantile Regression*. Cambridge University Press.

Kowal, D. R., Bravo, M., Leong, H., Bui, A., Griffin, R. J., Ensor, K. B., and Miranda, M. L. (2021). Bayesian variable selection for understanding mixtures in environmental exposures. *Statistics in Medicine*, 40:4850–4871.

Linero, A. R. and Daniels, M. J. (2018). Bayesian approaches for missing not at random outcome data: the role of identifying restrictions. *Statistical Science*, 33:198–213.

Miller, J. W. and Dunson, D. B. (2018). Robust Bayesian inference via coarsening. *Journal of the American Statistical Association*, 114:1113–1125.

Miranda, M. L., Kim, D., Reiter, J. P., Overstreet Galeano, M. A., and Maxson, P. (2009). Environmental contributors to the achievement gap. *Neurotoxicology*, 30:1019–1024.

Molenberghs, G., Beunckens, C., Sotto, C., and Kenward, M. G. (2008). Every missingness not at random model has a missingness at random counterpart with equal fit. *Journal of the Royal Statistical Society, Series B*, 70:371–378.

Murray, J. S., Dunson, D. B., Carin, L., and Lucas, J. E. (2013). Bayesian Gaussian

copula factor models for mixed data. *Journal of the American Statistical Association*, 108:656–665.

Pham, T. M., Carpenter, J. R., Morris, T. P., Wood, A. M., and Petersen, I. (2018). Population-calibrated multiple imputation for a binary/categorical covariate in categorical regression models. *Statistics in Medicine*, 38:792–808.

Pitt, M., Chan, D., and Kohn, R. (2006). Efficient Bayesian inference for Gaussian copula regression models. *Biometrika*, 93(3):537–554.

Rubin, D. B. (1976). Inference and missing data. *Biometrika*, 63:581—592.

Rubin, D. B. (1987). *Multiple Imputation for Nonresponse in Surveys*. New York: John Wiley.

Sadinle, M. and Reiter, J. P. (2017). Itemwise conditionally independent nonresponse modelling for incomplete multivariate data. *Biometrika*, 104:207–220.

Sadinle, M. and Reiter, J. P. (2019). Sequentially additive nonignorable missing data modelling using auxiliary marginal information. *Biometrika*, 106:889–911.

Si, Y., Reiter, J. P., and Hillygus, D. S. (2015). Semi-parametric selection models for potentially non-ignorable attrition in panel studies with refreshment samples. *Political Analysis*, 23:92–112.

Si, Y., Reiter, J. P., and Hillygus, D. S. (2016). Bayesian latent pattern mixture models for handling attrition in panel studies with refreshment samples. *Annals of Applied Statistics*, 10:118–143.

Tang, J., Hillygus, D. S., and Reiter, J. P. (2024). Using auxiliary marginal distributions

in imputations for nonresponse while accounting for survey weights, with application to estimating voter turnout. *Journal of Survey Statistics and Methodology*, 12:155–182.

van Buuren, S. (2018). *Flexible Imputation of Missing Data*. Chapman & Hall/CRC Press.

Zhao, Y. and Udell, M. (2020). Missing value imputation for mixed data via Gaussian copula. In *Proceedings of the 26th ACM SIGKDD International Conference on Knowledge Discovery & Data Mining*, pages 636–646.

Supplement to
“Gaussian Copula Models for Nonignorable Missing Data Using
Auxiliary Marginal Quantiles”

A Introduction

This document includes supplementary material to the main text. Section B outlines the Gibbs sampler for use with full marginal specifications in \mathcal{A} . Section C includes the proofs of the theorems from the main text. Section D presents the extension of the Gaussian copula model to handle unordered categorical variables. Section E presents the full model specification for the EQL and EHQL including the prior distributions from the factor model described in the main text, as well as the full conditional distributions used in the Gibbs samplers for those models. Section F presents results of additional simulations. Section G presents additional results from the analysis of the North Carolina lead data.

B Gibbs Sampler for Full Marginal Specifications

Given a set $\{F_j\}_{j=1}^p$ of fully specified marginal distributions for the study variables, we use Algorithm 3 to sample from the posterior distribution of $(\mathbf{C}_\theta, \boldsymbol{\alpha})$ and impute \mathbf{y}^{mis} . We presume the analyst uses the prior distribution described in Section 4 of the main text. In the algorithm, the subscript $(-j)$ in a vector denotes that vector without the j th element; the subscript $(-j)$ in the column (row) index of a matrix indicates exclusion of the elements

Algorithm 3 Bayesian estimation and imputation for the Gaussian copula with fixed marginals.

Require: prior $p(\mathbf{C}_\theta, \boldsymbol{\alpha})$, marginals $\{F_j\}_{j=1}^p$. Let $\mathbf{C} = \mathbf{C}_\theta$.

- **Step 1:** Sample $(\mathbf{z}^{mis}, \mathbf{z}_r) | \mathbf{C}, \boldsymbol{\alpha}$

for $j \in \{1, \dots, 2p\}$ do

Compute $\mu_{ij} = \alpha_j + \mathbf{C}_{j(-j)} \mathbf{C}_{-(jj)}^{-1} (\mathbf{z}_{i(-j)} - \boldsymbol{\alpha}_{-j})$ and $\sigma_j^2 = \mathbf{C}_{jj} - \mathbf{C}_{j(-j)} \mathbf{C}_{-(jj)}^{-1} \mathbf{C}_{(-j)j}$

if $z_{ij} \in \mathbf{z}_r$ then

$\ell_{ij} = 0 - \infty \mathbb{1}_{r_j=1}$, $u_{ij} = 0 + \infty \mathbb{1}_{r_j=0}$

Sample $z_{ij} \sim \text{Normal}(\mu_{ij}, \sigma_j^2) \mathbb{1}(\ell_{ij}, u_{ij})$

if $z_{ij} \in \mathbf{z}^{mis}$ then

Sample $z_{ij} \sim \text{Normal}(\mu_{ij}, \sigma_j^2)$

- **Step 2:** Sample $\mathbf{C}, \boldsymbol{\alpha} \sim p(\mathbf{C}, \boldsymbol{\alpha} | \mathbf{z}^{obs}, \mathbf{z}^{mis}, \mathbf{z}_r)$

where $p(\mathbf{C}, \boldsymbol{\alpha} | \mathbf{z}^{obs}, \mathbf{z}^{mis}, \mathbf{z}_r) \propto N_{2p}((\mathbf{z}^{obs}, \mathbf{z}^{mis}, \mathbf{z}_r); \boldsymbol{\alpha}, \mathbf{C}) p(\mathbf{C}, \boldsymbol{\alpha})$

- **Step 3:** Impute $y_{ij}^{mis} = F_j^{-1}(\Phi(z_{ij}^{mis}))$

corresponding to the j th column (row) of that matrix; and, the subscript $-(jj)$ in a matrix indicates exclusion of all row and column elements for the j th variable in that matrix. Algorithm 3 can be used generally when full marginal distributions are available.

C Proofs of Theorems in Main Text

In this section we present proofs of Theorem 1, Lemma 1, and Theorem 2 from the main text. In the proofs, equations referenced by number only, e.g., (2)–(3), refer to the corresponding equations in the main text.

Theorem 1. Suppose $\{(\mathbf{y}_i, \mathbf{r}_i)\}_{i=1}^n \stackrel{iid}{\sim} \Pi_0$ where Π_0 is the Gaussian copula with correlation \mathbf{C}_0 and marginals $\{F_j\}_{j=1}^p$ as in (2)–(3), and $\{\mathcal{A}_j\}_{j=1}^p = \{F_j\}_{j=1}^p$. Let $p(\boldsymbol{\theta})$ be a prior with respect a measure that induces a prior Π over the space of all $2p \times 2p$ correlation matrices \mathbb{C} with $\Pi(\mathbf{C}_\theta) > 0$ for all $\mathbf{C}_\theta \in \mathbb{C}$. Then, for all $\epsilon > 0$, $\lim_{n \rightarrow \infty} \Pi_n\{\mathcal{U}_\epsilon(\mathbf{C}_0)\} \rightarrow 1$ almost surely $[\Pi_0]$, where $\mathcal{U}_\epsilon(\mathbf{C}_0) = \{\mathbf{C}_\theta \in \mathbb{C} : \|\mathbf{C}_0 - \mathbf{C}_\theta\|_F < \epsilon\}$ and $\|\cdot\|_F$ is Frobenius norm.

Proof. Without loss of generality, suppose $\boldsymbol{\alpha} = \mathbf{0}$. Let $f_n(\mathbf{C}_\theta) = -n^{-1} \sum_{i=1}^n \log p(\mathbf{z}_i^{obs}, \mathbf{z}_{\mathbf{r}_i} | \mathcal{E}(\mathbf{r}_i); \mathbf{C}_\theta)$ computed with the n sampled draws of $(\mathbf{y}_i^{obs}, \mathbf{r}_i)$. Here, $\mathcal{E}(\mathbf{r}_i)$ is the probit set restriction defined in the main text specific to the values of the nonresponse indicators \mathbf{r}_i .

Let $(\mathbf{Z}^{obs}, \mathbf{Z}_R)$ represent the latent random variables for a random draw of $(\mathbf{y}^{obs}, \mathbf{r})$ from Π_0 . Define $f(\mathbf{C}_\theta) = -\mathbb{E}_{\Pi_0} \log p(\mathbf{Z}^{obs}, \mathbf{Z}_R \in \mathcal{E}(\mathbf{R}); \mathbf{C}_\theta)$, where the expectation is with respect to Π_0 with known $\mathcal{A} = \{F_j\}_{j=1}^p$ and $\mathcal{E}(\mathbf{R})$ is the probit set restriction corresponding to the random draw of \mathbf{r} . Let $\phi_{\mathbf{C}_\theta}$ and $\phi_{\mathbf{C}_0}$ represent the $2p$ -dimensional multivariate Gaussian densities with correlation \mathbf{C}_θ and \mathbf{C}_0 , respectively.

The proof establishes that the following conditions from Theorem 3 in Miller (2021) hold almost surely $[\Pi_0]$:

1. $\Pi\{\mathcal{U}_\epsilon(\mathbf{C}_0)\} > 0$;
2. $f_n \rightarrow f$ pointwise on \mathbb{C} ;
3. f_n is convex for each n ;
4. $\mathbb{C} \subseteq \mathbb{R}^{2p(2p-1)}$;
5. $\mathbf{C}_0 \in \text{int}(\mathbb{C})$; and
6. $f(\mathbf{C}_\theta) > f(\mathbf{C}_0)$ for all $\mathbf{C}_\theta \in \mathbb{C} \setminus \mathbf{C}_0$.

Conditions 1, 4, and 5 are satisfied directly by the theorem assumptions on the prior Π . Condition 3 is satisfied since $p(\mathbf{z}_i^{obs}, \mathbf{z}_{\mathbf{r}_i} \in \mathcal{E}(\mathbf{r}_i); \mathbf{C}_\theta)$ is a function of the Gaussian density which is log concave. Condition 2 is satisfied by the strong law of large numbers and since each $(\mathbf{y}_i, \mathbf{r}_i)$, where $i = 1, \dots, n$, is an i.i.d. sample from Π_0 .

To validate condition 6, we first establish the Kullback-Leibler (KL) divergence between $\Pi_{\mathbf{C}_\theta}^{obs} = p(\mathbf{y}^{obs}, \mathbf{r} \mid \mathbf{C}_\theta, \{F_j\}_{j=1}^p)$ for $\mathbf{C}_\theta \in \mathbb{C}$ and the distribution of the observed data given the ground truth copula correlation, $\Pi_0^{obs} = p(\mathbf{y}^{obs}, \mathbf{r} \mid \mathbf{C}_0, \{F_j\}_{j=1}^p)$. Here, the KL-divergence between distributions P and Q with density functions p and q , respectively, is given by $d_{KL}(P, Q) = \int p(\mathbf{x}) \log\{p(\mathbf{x})/q(\mathbf{x})\} d\mathbf{x}$.

To begin, let \mathbf{r}^g be one of the 2^p possible combinations of (R_1, \dots, R_p) , with $\mathcal{E}(\mathbf{r}^g)$ the associated probit set restriction for \mathbf{z}_r when $\mathbf{r} = \mathbf{r}^g$. For example, for two study variables consider $\mathbf{r}^g = (R_1 = 1, R_2 = 1)$. For arbitrary \mathbf{C}_θ , we write the marginal probability $p(\mathbf{R} =$

$\mathbf{r}^g) = \int_{\mathbf{z}_r \in \mathcal{E}(\mathbf{r}^g)} \phi_{\mathbf{C}_\theta}(\mathbf{z}_r) d\mathbf{z}_r = \int_0^\infty \int_0^\infty \phi_{\mathbf{C}_\theta}(z_1, z_2) dz_1 dz_2$. The set restriction $\mathcal{E}(\mathbf{r}^g)$ implied by the collection of unique missingness patterns in \mathbf{r}^g covers a non-overlapping orthant in the p -dimensional latent space for \mathbf{z}_r . Thus, we have $\bigcup_{g=1}^{2^p} \mathcal{E}(\mathbf{r}^g) = \sum_{g=1}^{2^p} \mathcal{E}(\mathbf{r}^g) = \mathbb{R}^p$. Illustrating this with the two-dimensional example above, we observe that $\sum_{g=1}^{2^2} \int_{\mathbf{z}_r \in \mathcal{E}(\mathbf{r}^g)} \phi_{\mathbf{C}_\theta}(\mathbf{z}_r) d\mathbf{z}_r = \int_{-\infty}^\infty \int_{-\infty}^\infty \phi_{\mathbf{C}_\theta}(\mathbf{z}_r) d\mathbf{z}_r$. Thus, for p -dimensional \mathbf{z}_r , we may express the expectation of $g(\mathbf{z}_r)$ for some function g as

$$\sum_{g=1}^{2^p} \int_{\mathbf{z}_r \in \mathcal{E}(\mathbf{r}^g)} g(\mathbf{z}_r) \phi_{\mathbf{C}_\theta}(\mathbf{z}_r) d\mathbf{z}_r = \int_{\mathbb{R}^p} g(\mathbf{z}_r) \phi_{\mathbf{C}_\theta} d\mathbf{z}_r \quad (\text{C.1})$$

Consequently, with known marginals, we leverage the simplification of the Gaussian copula likelihood in (4)–(5) to express $d_{KL}(\Pi_0^{obs}, \Pi_{\mathbf{C}_\theta}^{obs})$ as

$$d_{KL}(\Pi_0^{obs}, \Pi_{\mathbf{C}_\theta}^{obs}) = \sum_{g=1}^{2^p} \int p(\mathbf{y}^{obs}, \mathbf{r}^g \mid \mathbf{C}_0, \{F_j\}_{j=1}^p) \log \left\{ \frac{p(\mathbf{y}^{obs}, \mathbf{r}^g \mid \mathbf{C}_0, \{F_j\}_{j=1}^p)}{p(\mathbf{y}^{obs}, \mathbf{r}^g \mid \mathbf{C}_\theta, \{F_j\}_{j=1}^p)} \right\} d\mathbf{y}^{obs} \quad (\text{C.2})$$

$$= \sum_{g=1}^{2^p} \int \int \int_{\mathbf{z}_r \in \mathcal{E}(\mathbf{r}^g)} \phi_{\mathbf{C}_0}(\mathbf{z}^{obs}, \mathbf{z}^{mis}, \mathbf{z}_r) \log \left\{ \frac{\phi_{\mathbf{C}_0}(\mathbf{z}^{obs}, \mathbf{z}^{mis}, \mathbf{z}_r)}{\phi_{\mathbf{C}_\theta}(\mathbf{z}^{obs}, \mathbf{z}^{mis}, \mathbf{z}_r)} \right\} d\mathbf{z}^{obs} d\mathbf{z}^{mis} d\mathbf{z}_r \quad (\text{C.3})$$

$$= \int \int \int \phi_{\mathbf{C}_0}(\mathbf{z}^{obs}, \mathbf{z}^{mis}, \mathbf{z}_{r'}) \log \left\{ \frac{\phi_{\mathbf{C}_0}(\mathbf{z}^{obs}, \mathbf{z}^{mis}, \mathbf{z}_r)}{\phi_{\mathbf{C}_\theta}(\mathbf{z}^{obs}, \mathbf{z}^{mis}, \mathbf{z}_r)} \right\} d\mathbf{z}^{obs} d\mathbf{z}^{mis} d\mathbf{z}_r. \quad (\text{C.4})$$

The equivalence between (C.2) and (C.3) arises from (4)–(5) in the main text: with the margins known, the transformation between \mathbf{y}^{obs} and \mathbf{z}^{obs} is fixed. In addition, since $\bigcup_{g=1}^{2^p} \mathcal{E}(\mathbf{r}^g) = \mathbb{R}^p$, we may collapse the sum into an integral which leads to the equivalence between (C.3) and (C.4).

Consequently, the KL-divergence between Π_0^{obs} and $\Pi_{\mathbf{C}_\theta}^{obs}$ when the margins are known reduces to evaluating the KL divergence between $2p$ -dimensional multivariate Gaussian distributions. It is well known that

$$d_{KL}(\Pi_0^{obs}, \Pi_{\mathbf{C}_\theta}^{obs}) = \frac{1}{2} \left\{ \text{tr}(\mathbf{C}_\theta^{-1} \mathbf{C}_0) - 2p + \log \left(\frac{|\mathbf{C}_\theta|}{|\mathbf{C}_0|} \right) \right\}. \quad (\text{C.5})$$

This quantity is minimized when $\mathbf{C}_\theta = \mathbf{C}_0$, in which case $d_{KL}(\Pi_0^{obs}, \Pi_{\mathbf{C}_\theta}^{obs}) = 0$. By construction, $\mathbf{C}_\theta = \mathbf{C}_0$ also minimizes $f(\mathbf{C}_\theta)$. Therefore, $f(\mathbf{C}_\theta) > f(\mathbf{C}_0)$ for all $\mathbf{C}_\theta \in \mathbb{C} \setminus \mathbf{C}_0$. \square

Lemma 1. Suppose $\{(\mathbf{y}_i, \mathbf{r}_i)\}_{i=1}^n \stackrel{iid}{\sim} \Pi_0$ where Π_0 is the Gaussian copula with correlation \mathbf{C}_0 and marginals $\{F_j\}_{j=1}^p$ as in (2)–(3), and $\{\mathcal{A}_j\}_{j=1}^p = \{F_j\}_{j=1}^p$. For any value of $(\mathbf{y}_i^{obs}, \mathbf{y}_i^{mis})$, $p(R_{ij} = 1 \mid \mathbf{y}_i^{obs}, \mathbf{y}_i^{mis}, \mathbf{C}_j^*, \alpha_{r_j}, \{F_j\}_{j=1}^p)$ satisfies (10) with $x_{ik} = z_{ik}$, g the probit link function in (8)–(9), $\beta_0 = \alpha_{r_j}$, and β_k the k th component of the vector $\mathbf{C}_{r_j \mathbf{y}} \mathbf{C}_{\mathbf{y}}^{-1}$.

Proof. The probit restriction implies that $Z_{R_{ij}} > 0$ when $R_{ij} = 1$. Therefore,

$$p(R_{ij} = 1 \mid \mathbf{y}_i^{obs}, \mathbf{y}_i^{mis}, \mathbf{C}_j^*, \alpha_{r_j}, \{F_j\}_{j=1}^p) = p(Z_{R_{ij}} > 0 \mid \mathbf{z}_i^{mis}, \mathbf{z}_i^{obs}, \mathbf{C}_j^*, \alpha_{r_j}) \quad (\text{C.6})$$

$$= 1 - \Phi_{\alpha_{ij}^*, \sigma_j^{2*}}(0) \quad (\text{C.7})$$

$$= 1 - \Phi_{0, \sigma_j^{2*}}(\alpha_{ij}^*). \quad (\text{C.8})$$

Here, we have

$$\alpha_{ij}^* = \alpha_{r_j} + \mathbf{C}_{r_j \mathbf{y}} \mathbf{C}_{\mathbf{y}}^{-1} \mathbf{z}_i \quad (\text{C.9})$$

$$= \alpha_{r_j} + \sum_{k=1}^p \sum_{j=1}^p \mathbf{C}_{r_j y_j} \mathbf{C}_{y_k y_j}^{-1} z_{ij} \quad (\text{C.10})$$

$$= \alpha_{r_j} + \sum_{j=1}^p \beta_j z_{ij}. \quad (\text{C.11})$$

Consequently, the mean of (C.8) is additive in the components of \mathbf{z}_i , which implies that $p(R_{ij} = 1 \mid \mathbf{y}_i^{obs}, \mathbf{y}_i^{mis}, \mathbf{C}_j^*, \alpha_{r_j}, \{F_j\}_{j=1}^p)$ satisfies (10) with the probit link function. \square

Theorem 2. Suppose $\{(\mathbf{y}_i, \mathbf{r}_i)\}_{i=1}^n \stackrel{iid}{\sim} \Pi_0$ where Π_0 is the Gaussian copula with correlation \mathbf{C}_0 and marginals $\{F_j\}_{j=1}^p$ as in (2)–(3). For $j = 1, \dots, p$, suppose \mathcal{A}_j comprises $m_j \geq 3$ auxiliary quantiles of F_j , including $F_j^{-1}(0)$ and $F_j^{-1}(1)$. Let $p(\theta)$ be a prior with respect a measure that induces a prior Π over the space of all $2p \times 2p$ correlation matrices \mathbb{C} such that

$\Pi(\mathbf{C}_\theta) > 0$ for all $\mathbf{C}_\theta \in \mathbb{C}$. Then, for any neighborhood \mathcal{B} of \mathbf{C}_0 , $\lim_{n \rightarrow \infty} \Pi_n^*(\mathbf{C}_\theta \in \mathcal{B}) \rightarrow 1$ almost surely $[\Pi_0]$.

Proof. We prove this result using a variant of Doob's theorem presented in Gu and Ghosal (2009).

Doob's Theorem *Let X_i be observations whose distributions depend on a parameter θ , both taking values in Polish spaces. Assume $\theta \sim \Pi$ and $X_i | \theta \sim P_\theta$. Let \mathcal{X}_N be the σ -field generated by X_1, \dots, X_N , and $\mathcal{X}_\infty = \sigma(\bigcup_i^\infty \mathcal{X}_i)$. If there exists a \mathcal{X}_∞ measurable function f such that for $(\omega, \theta) \in \Omega^\infty \times \Theta$, $\theta = f(\omega)$ a.e. $[P_\theta^\infty \times \Pi]$ then the posterior is strongly consistent at θ for almost every θ $[\Pi]$.*

For $j = 1, \dots, p$, let B_j be the ordinal random variable with $m_j - 1$ levels resulting from the coarsening of Y_j from the intervals in (12). Let R_j be the random variable corresponding to the process of nonresponse for Y_j . Because of Doob's theorem, it suffices to show that, for any pair of $(B_j, B_{j'})$, $(B_j, R_{j'})$, or $(R_j, R_{j'})$, we can recover the true copula correlation $\rho_{0,jj'}$ between the pair of variables by a function that is measurable with respect to the σ -field generated by the sequence of $\{\mathbf{z}^{obs} \in \mathcal{D}(\mathbf{b}^{obs}), \mathbf{z}_r \in \mathcal{E}(\mathbf{r})\}$ as $n \rightarrow \infty$.

We first note that the marginal distribution of any B_j is fully specified by \mathcal{A}_j . To see this, for any level $q = 1, \dots, m_j - 1$ with $B_j = q$ defined as in (12), the marginal probability is exactly $p(B_j = q) = p(Z_j \in (\Phi^{-1}(\tau_j^q), \Phi^{-1}(\tau_j^{q+1}))]) = \tau_j^{q+1} - \tau_j^q$. Furthermore, $\sum_{q=1}^{m_j-1} p(B_j = q) = \sum_{q=1}^{m_j-1} \tau_j^{q+1} - \tau_j^q = 1$, since $\tau_j^{m_j} = 1$ and $\sum_{q=1}^{m_j-1} \tau_j^{q+1} - \tau_j^q$ is a telescoping series. Thus, \mathcal{A}_j provides the entire marginal distribution function of B_j .

We next consider the joint distributions arising from the three combinations of binned study variables and missingness indicators for any $j, j' \in \{1, \dots, p\}$. The joint distribution for $(B_j, B_{j'})$, where $j \neq j'$, can be represented by a contingency table concatenated to a $m_j m_{j'} \times 1$ vector $\boldsymbol{\pi}_{B_j, B_{j'}} = \{\pi_{qk} : q = 1, \dots, m_j; k = 1, \dots, m_{j'}\}$, where any $\pi_{qk} = p(B_j = q, B_{j'} = k)$. Similarly, we can define $\boldsymbol{\pi}_{B_j, R_{j'}} = \{\pi_{qk} : q = 1, \dots, m_j; k = 0, 1\}$ where $\pi_{qk} = p(B_j = q, R_{j'} = k)$. And, for $j \neq j'$, we can define $\boldsymbol{\pi}_{R_j, R_{j'}} = \{\pi_{qk} : q = 0, 1; k = 0, 1\}$

where $\pi_{qk} = p(R_j = q, R_{j'} = k)$. By construction, we have that $p(B_j = q) = p(Y_j \in \mathcal{I}_j^q)$, and so any of the joint probabilities above involving B_j may be expressed in terms of Y_j . Since $\{(\mathbf{y}_i, \mathbf{r}_i)\}_{i=1}^n$ come from a Gaussian copula with correlation \mathbf{C}_0 , and any pair of variables also follows a Gaussian copula with sub-correlation $\rho_{0,jj'}$, we may express the joint distributions in terms of the data generating Gaussian copula parameters. For example,

$$p(B_j = q, B_{j'} = k) = p(Y_j \in \mathcal{I}_j^q, Y_{j'} \in \mathcal{I}_{j'}^k) \quad (\text{C.12})$$

$$= \int_{\Phi^{-1}(\tau_j^q)}^{\Phi^{-1}(\tau_j^{q+1})} \int_{\Phi^{-1}(\tau_{j'}^k)}^{\Phi^{-1}(\tau_{j'}^{k+1})} \phi(z_j, z_{j'}; \rho_{0,jj'}) dz_j dz_{j'}. \quad (\text{C.13})$$

For notational convenience, we drop the subscripts from $\boldsymbol{\pi}_{B_j, B_{j'}}$, $\boldsymbol{\pi}_{B_j, R_{j'}}$, and $\boldsymbol{\pi}_{R_j, R_{j'}}$ and let $\boldsymbol{\pi}$ be defined in context.

We consider three types of sequences of empirical contingency tables. For pairs $(B_j, B_{j'})$, the sequence is $\boldsymbol{\pi}^n$ with entries $\pi_{qk}^n = n^{-1} \sum_{i=1}^n \mathbb{1}(B_{ij} = q, B_{ij'} = k)$. Re-using π_{qk}^n for economy of notation, for pairs $(R_j, R_{j'})$, the sequence has entries $\pi_{qk}^n = n^{-1} \sum_{i=1}^n \mathbb{1}(R_{ij} = q, R_{ij'} = k)$. Finally, for pairs $(B_j, R_{j'})$, the sequence has entries $\pi_{qk}^n = n^{-1} \sum_{i=1}^n \mathbb{1}(B_{ij} = q, R_{ij'} = k)$. Note that we may construct $\boldsymbol{\pi}^n$ from the information contained in any realization of $\{\mathbf{z}^{obs} \in \mathcal{D}(\mathbf{b}^{obs}), \mathbf{z}_r \in \mathcal{E}(\mathbf{r})\}$ by simply observing the counts falling into corresponding intervals specified by \mathcal{A} or the probit restrictions on the R_j . Therefore, the σ -field generated by the sequence of $\boldsymbol{\pi}^n$ is a sub σ -field of that generated by the sequence of $\{\mathbf{z}^{obs} \in \mathcal{D}(\mathbf{b}^{obs}), \mathbf{z}_r \in \mathcal{E}(\mathbf{r})\}$. Thus, any function that is measurable with respect to the σ -field generated by the sequence of $\boldsymbol{\pi}^n$ is also measurable with respect to that generated by the sequence of $\{\mathbf{z}^{obs} \in \mathcal{D}(\mathbf{b}^{obs}), \mathbf{z}_r \in \mathcal{E}(\mathbf{r})\}$. We will work exclusively with the former.

We proceed to show that for any pair of variables among $\{B_1, \dots, B_p, R_1, \dots, R_p\}$, each entry in $\boldsymbol{\pi}^n$ is identified by the observed (coarsened) data. As a consequence of the model for $\{(\mathbf{y}_i, \mathbf{r}_i)\}_{i=1}^n$, we show that $\boldsymbol{\pi}^n \xrightarrow{a.s.} \boldsymbol{\pi}$. We then show that there exists an estimator $\hat{\rho}_{jj'}$ which may be obtained by a function that is measurable with respect to the σ -field generated by the sequence of $\boldsymbol{\pi}_n$. This estimator must converge to a limit, $\rho_{jj'}^*$, which is therefore measurable

with respect to the σ -field generated by the infinite sequence of $\boldsymbol{\pi}_n$. Finally, we show that $\rho_{jj'}^* = \rho_{0,jj'}$ which concludes the proof.

We first consider $\boldsymbol{\pi}^n$ constructed from $(R_j, R_{j'})$. Since each R_{ij} is always observed, it is immediately apparent through the strong law of large numbers (S.L.L.N.) that $\boldsymbol{\pi}^n \xrightarrow{a.s.} \boldsymbol{\pi}$.

For $\boldsymbol{\pi}^n$ constructed using $(B_j, R_{j'})$, we first utilize theory on the additive nonignorable missingness mechanism along with the identifying information for B_j to demonstrate that $\boldsymbol{\pi}^n$ is identified by the observed data. We have the following equivalences under the data generating Gaussian copula.

$$p(B_j = q, R_{j'} = 1) = p(B_j = q)p(R_{j'} = 1 \mid B_j = q) \quad (\text{C.14})$$

$$= p(Y_j \in \mathcal{I}_j^q)p(R_{j'} = 1 \mid Y_j \in \mathcal{I}_j^q) \quad (\text{C.15})$$

$$= p(Z_j \in (\Phi^{-1}(\tau_j^q), \Phi^{-1}(\tau_j^{q+1}]))p(Z_{R_{j'}} > 0 \mid Z_j \in (\Phi^{-1}(\tau_j^q), \Phi^{-1}(\tau_j^{q+1}))). \quad (\text{C.16})$$

The first term in (C.16) is known since the marginal distribution of B_j is fully specified from \mathcal{A}_j . To characterize the missingness mechanism implied by the second term, we require theory on the selection normal distribution (Arellano-Valle and Azzalini, 2006), given in Lemma (2).

Lemma 2. *Suppose $(\mathbf{x}_0, \mathbf{x}_1)$ are jointly Gaussian such that $\mathbf{X}_0 \sim N_p(\boldsymbol{\mu}_0, \boldsymbol{\Sigma}_0)$ and $\mathbf{X}_1 \sim N_{p^*}(\boldsymbol{\mu}_1, \boldsymbol{\Sigma}_1)$ with joint covariance matrix $\boldsymbol{\Sigma} = \begin{bmatrix} \boldsymbol{\Sigma}_0 & \boldsymbol{\Sigma}_{01} \\ \boldsymbol{\Sigma}_{10} & \boldsymbol{\Sigma}_1 \end{bmatrix}$. Define $\mathbf{X}_0^{(\mathcal{C})} \stackrel{d}{=} [\mathbf{X}_0 \mid \mathbf{X}_0 \in \mathcal{C}]$ for \mathcal{C} some p -dimensional hypercube. Then, $[\mathbf{X}_1 \mid \mathbf{X}_0 \in \mathcal{C}] \stackrel{d}{=} \boldsymbol{\mu}_0 + \mathbf{X}_1 + \boldsymbol{\Sigma}_{10}^T \boldsymbol{\Sigma}_0^{-1} \mathbf{X}_0^{(\mathcal{C})}$, and we say that $[\mathbf{X}_1 \mid \mathbf{X}_0 \in \mathcal{C}] \sim \text{SLCT-}N_{p,p^*}(\boldsymbol{\mu}_0, \boldsymbol{\mu}_1, \boldsymbol{\Sigma}_0, \boldsymbol{\Sigma}_1, \boldsymbol{\Sigma}_{01}, \mathcal{C})$.*

Setting $\mathcal{C} = (\Phi^{-1}(\tau_j^q), \Phi^{-1}(\tau_j^{q+1}))$ we observe from (C.16) that $[Z_{R_{j'}} \mid Z_j \in \mathcal{C}] \sim \text{SLCT-}N_{1,1}(\alpha_{R_j}, 0, 1, 1, \rho_{0,jj})$. This distribution satisfies the requisite properties of a link function outlined in Lemma 1. Furthermore, the construction $[\mathbf{X}_1 \mid \mathbf{X}_0 \in \mathcal{C}] \stackrel{d}{=} \boldsymbol{\mu}_0 + \mathbf{X}_1 + \boldsymbol{\Sigma}_{10}' \boldsymbol{\Sigma}_0^{-1} \mathbf{X}_0^{(\mathcal{C})}$ of SLCT-N random variables demonstrates that this missingness mechanism is additive in $Z_j \in \mathcal{C}$, with $\beta = \rho_{0,jj'}$. Using the equivalence between (C.14) and (C.16), to-

gether with the fact that the marginal distribution of B_j is completely specified, by Theorem 1 of Sadinle and Reiter (2019) this establishes that each component of $\boldsymbol{\pi}^n$ is identified by the observed data. Furthermore, due to the correspondence between $(B_j, R_{j'})$ and $(Y_j, R_{j'})$, and since $(Y_j, R_{j'})$ are distributed according to a Gaussian copula with correlation $\rho_{0,jj'}$, the identified probability π_{qk}^n must converge to π_{qk} generated by the true copula by the S.L.L.N. Applying this to each entry of the vector we have $\boldsymbol{\pi}^n \xrightarrow{a.s.} \boldsymbol{\pi}$ for any pair $(B_j, R_{j'})$.

For $\boldsymbol{\pi}^n$ constructed using $(B_j, B_{j'})$, we use similar logic as used for $(B_j, R_{j'})$. We first consider the joint probability, $p(B_j = q, B_{j'} = k, R_j = 1, R_{j'} = 1)$. This may be written as

$$\begin{aligned} & p(B_j = q, B_{j'} = k, R_j = 1, R_{j'} = 1) \\ &= p(B_j = q, B_{j'} = k)p(R_j = 1, R_{j'} = 1 \mid B_j = q, B_{j'} = k). \end{aligned} \quad (\text{C.17})$$

Of course, this decomposition holds for any combination in the sample space of $(B_j, B_{j'}, R_j, R_{j'})$. We can expand the joint missingness mechanism in (C.17) as

$$\begin{aligned} & p(R_j = 1, R_{j'} = 1 \mid B_j = q, B_{j'} = k) \\ &= p(R_j = 1 \mid B_j = q, B_{j'} = k)p(R_{j'} = 1 \mid B_{j'} = q, B_j = k, R_j = 1) \end{aligned} \quad (\text{C.18})$$

$$= p(Z_{R_j} > 0 \mid Z_j \in \mathcal{C}, Z_j \in \mathcal{C}')p(Z_{R_{j'}} > 0 \mid Z_j \in \mathcal{C}, Z_j \in \mathcal{C}', Z_{R_j} > 0), \quad (\text{C.19})$$

where $\mathcal{C} = (\Phi^{-1}(\tau_j^q), \Phi^{-1}(\tau_j^{q+1}))$ and $\mathcal{C}' = (\Phi^{-1}(\tau_{j'}^k), \Phi^{-1}(\tau_{j'}^{k+1}))$. Thus, each term in (C.19) reveals an additive nonignorable missingness mechanism via SLCT-N random variables per Lemma 2. This form defines a sequential additive nonignorable missingness mechanism for multivariate nonignorable missing data (Sadinle and Reiter (2019), Definition 6). Since the marginal distributions of both B_j and $B_{j'}$ are fully specified by \mathcal{A}_j and $\mathcal{A}_{j'}$, and the joint missingness mechanism is sequentially additive nonignorable under a SLCT-N link, the conditions in Theorem 3 of Sadinle and Reiter (2019) are satisfied. Therefore, the joint probabilities $p(B_j, B_{j'}, R_j, R_{j'})$, and thus the $\boldsymbol{\pi}^n$, are identified from the observed data. As

in the $(B_j, R_{j'})$ case, the correspondence between $(B_j, B_{j'})$ and $(Y_j, Y_{j'})$ coupled with the true data generating model enables application of the S.L.L.N. to conclude that $\boldsymbol{\pi}^n \xrightarrow{a.s.} \boldsymbol{\pi}$ for any pair $(B_j, B_{j'})$.

Finally, any $\boldsymbol{\pi}^n$ arises from discretizing latent Gaussian variables at fixed cut-points given by \mathcal{A} and the probit restrictions on R . Thus, the problem of estimating $\rho_{jj'}$ from $\boldsymbol{\pi}^n$ reduces to estimating the polychoric correlation coefficient (Olsson, 1979). The resulting likelihood is a regular parametric family admitting a consistent estimator through maximum likelihood estimation (MLE). Therefore, the MLE $\hat{\rho}_{jj'}$ of the polychoric correlation coefficient estimated from $\boldsymbol{\pi}^n$ is measurable with respect the σ -field generated by the sequence of $\boldsymbol{\pi}^n$, and its limit as $n \rightarrow \infty$, denoted $\rho_{jj'}^*$, is measurable with respect to the σ -field generated by the infinite sequence of $\boldsymbol{\pi}^n$.

It remains to show that $\rho_{jj'}^* = \rho_{0,jj'}$. Suppose towards a contradiction that $\rho_{jj'}^* \neq \rho_{0,jj'}$. For $(B_j, B_{j'})$, by construction, the limiting polychoric correlation satisfies

$$\pi_{qk} = p(B_j = q, B_{j'} = k \mid \rho_{jj'}^*) \quad (\text{C.20})$$

$$= p(Y_j \in \mathcal{I}_j^q, Y_{j'} \in \mathcal{I}_{j'}^k \mid \rho_{jj'}^*) \quad (\text{C.21})$$

$$= p(z_j \in (\Phi^{-1}(\tau_j^q), \Phi^{-1}(\tau_j^{q+1}]), z_{j'} \in (\Phi^{-1}(\tau_{j'}^k), \Phi^{-1}(\tau_{j'}^{k+1}]); \rho_{jj'}^*) \quad (\text{C.22})$$

$$= \int_{\Phi^{-1}(\tau_j^q)}^{\Phi^{-1}(\tau_j^{q+1})} \int_{\Phi^{-1}(\tau_{j'}^k)}^{\Phi^{-1}(\tau_{j'}^{k+1})} \phi(z_j, z_{j'}; \rho_{jj'}^*) dz_j dz_{j'} \quad (\text{C.23})$$

$$\neq \int_{\Phi^{-1}(\tau_j^q)}^{\Phi^{-1}(\tau_j^{q+1})} \int_{\Phi^{-1}(\tau_{j'}^k)}^{\Phi^{-1}(\tau_{j'}^{k+1})} \phi(z_j, z_{j'}; \rho_{0,jj'}) dz_j dz_{j'}. \quad (\text{C.24})$$

This is a contradiction, since under Π_0 , $\pi_{qk} = \int_{\Phi^{-1}(\tau_j^q)}^{\Phi^{-1}(\tau_j^{q+1})} \int_{\Phi^{-1}(\tau_{j'}^k)}^{\Phi^{-1}(\tau_{j'}^{k+1})} \phi(z_j, z_{j'}; \rho_{0,jj'}) dz_j dz_{j'}$. We have shown the contradiction for joint probabilities involving $(B_j, B_{j'})$, but this construction holds for combinations of $(B_j, R_{j'})$ as well. Therefore, we conclude that $\rho_{jj'}^* = \rho_{0,jj'}$. Consequently, we have shown the existence of a consistent estimator of $\rho_{0,jj'}$ which is measurable with respect to the σ -field generated by the sequence of $\{\boldsymbol{\pi}^n\}_{n=1}^\infty$.

□

D Extensions for Unordered Categorical Variables

In the main text, we present the EQL and EHQL likelihoods for mixed count and continuous variables. We now describe how to incorporate unordered categorical variables with no missing or MCAR values. In this case, we need not include nonresponse indicators for the unordered categorical variables in the copula model, and we do not need auxiliary information about these variables in \mathcal{A} . We took this modeling approach for the analysis of the North Carolina lead exposure data. We leave to future research handling nonignorable missing data and incorporating known marginal information about unordered categorical variables.

We use a diagonal orthant (Johndrow et al., 2013) representation for the unordered categorical study variables. The basic idea is to model each unordered categorical Y_j with a set of binary indicators for the levels of Y_j , adding a restriction that for any individual only one of these indicators can equal one. Following the Gaussian copula, we include a latent variable for each binary indicator, carrying the restriction on the set of indicators to the set of latent variables.

Suppose we have $t < p$ unordered categorical variables among the p study variables. Without loss of generality, let Y_1, \dots, Y_t represent these t unordered categorical study variables, and let Y_{t+1}, \dots, Y_p represent the remaining study variables, which may be continuous or ordinal. For $j = 1, \dots, t$, each Y_j takes one of c_j levels, which we write as $\{1, \dots, c_j\}$. For any $y_{ij} = c \in \{1, \dots, c_j\}$, we define a diagonal orthant representation that encodes a vector of c_j binary variables, $\boldsymbol{\gamma}_j = (\gamma_{j1}, \dots, \gamma_{jc_j})$. For any individual's observed data, only one element in $(\gamma_1, \dots, \gamma_{c_j})$ equals one. For example, if $y_{ij} = 2$ and $c_j = 4$, then $\boldsymbol{\gamma}_j = (0, 1, 0, 0)$ for individual i . We refer to each individual's $\boldsymbol{\gamma}_j$ as $\boldsymbol{\gamma}_{ij} = (\gamma_{ij1}, \dots, \gamma_{ijc_j})$.

In lieu of a single latent variable Z_j for unordered categorical Y_j , we add c_j latent variables,

$(Z_{j1}, \dots, Z_{jc_j})$, to the copula model corresponding to each $\{\gamma_{j1}, \dots, \gamma_{jc_j}\}$. Thus, the copula model with t unordered categorical study variables includes $\sum_{j=1}^t c_j + (p-t)$ latent variables for the study variables. We refer to each individual's vector of latent values for Y_j as $\mathbf{z}_{ij} = (z_{ij1}, \dots, z_{ijc_j})$. Since these latent variables model indicators, we use the probit representation so that $z_{ijc} > 0$ when $\gamma_{ijc} = 1$ and $z_{ijc} < 0$ when $\gamma_{ijc} = 0$, for any j and c . We also add a restriction that only one of $(z_{ij1}, \dots, z_{ijc_j})$ for any individual can be positive. That is, for all individuals i and unordered categorical variables Y_j , we require for any c that

$$\{\gamma_{ijc} = 1, \gamma_{ijc'} = 0 \ \forall c' \neq c\} \implies \{z_{ijc} > 0, z_{ijc'} < 0 \ \forall c' \neq c\}. \quad (\text{D.1})$$

This representation avoids the need to select one level of Y_j as a reference group. Aggregating this representation across (Y_1, \dots, Y_t) , the observed categorical variables must satisfy the event

$$\mathcal{D}'(\mathbf{y}^{obs}) = \{\mathbf{z}^{obs} : \gamma_{ijc} = 1 \implies z_{ijc} > 0, z_{ijc'} < 0 \ \forall c' \neq c, j = 1, \dots, t\}. \quad (\text{D.2})$$

This representation is also recommended for ordinal variables with few levels (Feldman and Kowal, 2022).

To estimate the copula model when the data are comprised of mixed continuous, ordinal, and unordered categorical variables, we combine the EQL/EHQL event from the main text defined over (Y_{t+1}, \dots, Y_p) with the diagonal orthant probit event in (D.2). This combined event, which we write as $\mathcal{D}^*(\mathbf{b}^{obs}) \cup \mathcal{D}'(\mathbf{y}^{obs})$, is used in (13)–(14) in the main text. Posterior inference for \mathbf{C}_θ under the factor model of Section 4 in the main text requires simple modifications to Algorithm 1 of the main text, which are outlined in Section E. As with the specification of the model for \mathbf{z}_r corresponding to the indicators for R , we add a non-zero α_j term to the model for any indicator variable introduced into the model by the diagonal orthant probit representation.

E Model Specification and Gibbs Samplers for EQL and EHQL

E.1 Hierarchical Specification of the Factor Model

We provide a hierarchical specification of the latent factor model in Section 4 in the main text, which is used to estimate the copula correlation matrix \mathbf{C}_θ . For ease of notation and to match the setting of the simulations in Section 4 of the main text, we presume each Y_j is continuous or ordinal. Let λ_{jh} be the element in the j th row and h th column of the factor loadings matrix $\mathbf{\Lambda}$. When we include latent variables for missingness indicators for all p study variables, so that we have $2p$ variables in total, the model is given by

$$\begin{aligned} \delta_1 &\sim \text{Gamma}(a_1, 1), \delta_l \sim (a_2, 1), l \geq 2 \\ \xi_h &= \prod_{l=1}^h \delta_l, \quad \phi_{jh} \sim \text{Gamma}(\nu/2, \nu/2) \\ [\lambda_{jh} \mid \phi_{jh}, \xi_h] &\sim N(0, \phi_{jh}^{-1}, \xi_h^{-1}), \boldsymbol{\eta}_i \sim N_k(\mathbf{0}, \mathbf{I}_k), \alpha_j \sim N(0, 1), \sigma_j^{-2} \sim \text{Inverse Gamma}(a_\sigma, b_\sigma) \\ \mathbf{z}_i &= \boldsymbol{\alpha} + \mathbf{\Lambda} \boldsymbol{\eta}_i + \boldsymbol{\epsilon}_i, \quad \boldsymbol{\epsilon}_i \sim N_{2p}(\mathbf{0}, \boldsymbol{\Sigma}). \end{aligned}$$

We place a prior on each non-zero component α_j of $\boldsymbol{\alpha}$. These correspond to latent variables for each R_j . The prior for $\mathbf{\Lambda}$ adopts the global-local shrinkage structure from Bhattacharya and Dunson (2011), which encourages column-wise shrinkage for rank selection. By design, this ordered shrinkage prior reduces sensitivity to the choice of the rank of $\mathbf{\Lambda}$, which we label k , provided the rank is sufficiently large. In the simulation studies, we set $k = 2p$ to be full-rank, although our results were not sensitive to $k < 2p$. We set $a_1 = 2, a_2 = 3, \nu = 3, a_\sigma = 1, b_\sigma = 0.3$ for the simulation studies, as well as for the North Carolina data analysis.

When the observed data include binary variables, for example, a binary Y_j or a set of γ_j created by expressing multinomial variables using the diagonal orthant representation from Section D, the model also should include a prior distribution on the non-zero α_j for the latent Z_j corresponding to each binary variable. The α_j for any continuous or ordered

categorical Y_j remains set to zero.

In the North Carolina data analysis, the Gaussian copula model does not have $2p$ variables. Rather, we use 18 latent variables corresponding to the study variables used in the modeling, which include latent variables for the binary indicators for the unordered categorical variables per Section D. We also use one nonresponse indicator for blood-lead measurements. Thus, we have 19 latent variables in the copula model, with dimensions adjusted accordingly. We set $k = 19$ for the rank of Λ .

E.2 Gibbs Sampling for the EHQL Gaussian Copula

Bayesian estimation of the EHQL Gaussian copula involves sampling from the conditional distributions for the model parameters, latent variables, and marginal distributions per Algorithm 2 of the main text. Here, we assume that the auxiliary information set \mathcal{A}^* includes intermediate quantiles. We present the sampler for study variables that include binary variables, including the diagonal orthant representation of unordered categorical variables. We do not include an R_j for those variables; we do include R_j for continuous and ordinal variables. As discussed previously, this requires adding a non-zero α_j for each indicator variable with prior distribution as described in Section (E.1). Modeling unordered categorical variables as nonignorable under the copula model is an area for future research.

As such, let p^* be the dimension of the combined set of study variables and missingness indicators, with unordered categorical variables augmented with their diagonal orthant representation per Section D. We index the p^* variables with $j = 1, \dots, p^*$. Let k be the rank of Λ and dimension of latent factors η , which we index with h . Finally, we index the observations with $i = 1, \dots, n$.

We present the steps in the Gibbs sampler for the EHQL. Under the EQL, only two steps change. We describe these changes after presenting the EHQL sampler.

1. **Sample the factor model parameters:**

- $\lambda_{j-} | - \sim N_k((\mathbf{D}_j^{-1} + \sigma_j^{-2} \boldsymbol{\eta}^T \boldsymbol{\eta})^{-1} \boldsymbol{\eta}^T \sigma_j^{-2} (\mathbf{z}_j - \alpha_j), (\mathbf{D}_j^{-1} + \sigma_j^{-2} \boldsymbol{\eta}^T \boldsymbol{\eta})^{-1})$, where $\mathbf{D}_j^{-1} = \text{diag}(\phi_{j1}\xi_1, \dots, \phi_{jk}\xi_k)$, $\mathbf{z}_j = (z_{1j}, \dots, z_{nj})^T$, and $\boldsymbol{\eta} = (\boldsymbol{\eta}_1, \dots, \boldsymbol{\eta}_n)^T$, for $j = 1, \dots, p^*$.
- $\sigma_j^{-2} | - \sim \text{Gamma}(a_\sigma + \frac{n}{2}, b_\sigma + \frac{1}{2} \sum_{i=1}^n \sum_{h=1}^k (z_{ij} - (\alpha_j + \lambda_{jh}\eta_{ih}))^2)$, for $j = 1, \dots, p^*$.
- $\boldsymbol{\eta}_i | - \sim N_k(\mathbf{I}_k + (\boldsymbol{\Lambda}^T \boldsymbol{\Sigma}^{-1} \boldsymbol{\Lambda})^{-1} \boldsymbol{\Lambda}^T \boldsymbol{\Sigma}^{-1} (\mathbf{z}_i - \boldsymbol{\alpha}), (\mathbf{I}_k + \boldsymbol{\Lambda} \boldsymbol{\Sigma}^{-1} \boldsymbol{\Lambda})^{-1})$, where $\mathbf{z}_i = (z_{i1}, \dots, z_{ip^*})$, for $i = 1, \dots, n$.
- $\phi_{jh} | - \sim \text{Gamma}(\frac{\nu+1}{2}, \frac{\nu+\xi_h \lambda_{jh}^2}{2})$, for $j = 1, \dots, p^*$, $h = 1, \dots, k$.
- $\delta_1 | - \sim \text{Gamma}(a_1 + \frac{p^* k}{2}, 1 + \frac{1}{2} \sum_{h=1}^k \xi_h^{(1)} \sum_{j=1}^p \phi_{jh} \lambda_{jh}^2)$, and for $h \geq 2$.
- $\delta_h | - \sim \text{Gamma}(a_1 + \frac{p^*(k-h+1)}{2}, 1 + \frac{1}{2} \sum_{h=2}^k \xi_h^{(h)} \sum_{j=1}^p \phi_{jl} \lambda_{jh}^2)$, where $\xi_h^{(h)} = \prod_{w=h, w \neq h}^h \delta_w$, for $h = 1, \dots, k$.

2. Sample all α_j

For all j corresponding to binary study variables, missingness indicators, or diagonal orthant expanded unordered categorical variables, we sample α_j from

- $\alpha_j | - \sim N((n\sigma_j^{-2} + 1)^{-1} \sigma_j^{-2} \sum_{i=1}^n \sum_{h=1}^k (z_{ij} - \lambda_{jh}\eta_{ih}), (n\sigma_j^{-2} + 1)^{-1})$.

3. Sample $\mathbf{z}^{obs}, \mathbf{z}^{mis}, \mathbf{z}_r$

Given the conditional independence among the components of \mathbf{z}_i given $\boldsymbol{\eta}_i$, we sample components of \mathbf{z} corresponding to observed data points column-by-column, consistent with the ordering induced by the EHQL. For components of \mathbf{z}_i associated with missing values, no ordering is imposed, and only the diagonal orthant restriction for categorical variables is enforced.

- *Missing unordered categorical/binary data:* For z_{ijc}^{mis} corresponding to the c th level of categorical variable Y_j with c_j levels, we first calculate the predictive probability that $y_{ij}^{mis} = c$. To do so, we compute the categorical probabilities for each level in Y_j , using the diagonal orthant set restriction of Section D. That is, we calculate the probability that $z_{ijc}^{mis} > 0$ while the components of $z_{ijc'}^{mis} < 0$ for $c \neq c'$ corresponding

to the remaining levels. Explicitly, this is written

$$P(z_{ijc}^{mis} > 0, \{z_{ijc'}^{mis} < 0 : c' \neq c, c' = 1, \dots, c_j\} \mid -) \propto (E.1)$$

$$1 - \Phi(0; \sum_{h=1}^k \lambda_{ct} \eta_{ih}, \sigma_j^2) \prod_{c' \in \{c_1, \dots, c_j\}, c' \neq c} \Phi(0; \sum_{h=1}^k \lambda_{c'h} \eta_{ih}, \sigma_{c'}^2).$$

We sample y_{ij}^{mis} using these probabilities, with the resulting imputation used in the sampling of z_{ijc}^{mis} under the diagonal orthant set restriction in Section D. Let $\text{TN}(\mu, \sigma^2, a, b)$ denote a truncated univariate normal with mean μ , variance σ^2 , lower truncation a , and upper truncation b . The re-sampling step for any z_{ijc}^{mis} is given by

$$z_{ijc}^{mis} \sim \begin{cases} \text{TN}(\sum_{h=1}^k \lambda_{ct} \eta_{ih}, \sigma_j^2, 0, \infty), & y_{ij}^{mis} = c \\ \text{TN}(\sum_{h=1}^k \lambda_{ct} \eta_{ih}, \sigma_j^2, -\infty, 0), & y_{ij}^{mis} \neq c. \end{cases} \quad (E.2)$$

If Y_j is binary, the probability is instead given by $P(z_{ij}^{mis} > 0 \mid -) = 1 - \Phi(0; \sum_{h=1}^k \lambda_{jh} \eta_{ih}, \sigma_j^2)$, but the re-sampling step E.2 remains the same

- *Missing numeric data:* In this case, z_{ij}^{mis} is sampled from the unrestricted univariate Gaussian,

$$z_{ij}^{mis} \mid - \sim N(\sum_{h=1}^k \lambda_{jt} \eta_{ih}, \sigma_j^2). \quad (E.3)$$

- *Observed data:* For each j , sample z_{ij}^{obs} from a truncated normal, with lower and upper bounds for each observation specified by the EHQL/diagonal orthant probit restriction:

$$z_{ij}^{obs} \mid - \sim \text{TN}(\sum_{h=1}^k \lambda_{jt} \eta_{ih}, \ell_{ij}, u_{ij}). \quad (E.4)$$

For ordinal, count, and continuous variables, the truncation limits are

$$\ell_{ij} = \max\{\Phi^{-1}(\tau_{ij}^\ell), \max(z_{vj}^{obs} : z_{vj}^{obs} \in \mathcal{I}_j^{q-1}, v = 1, \dots, n)\} \quad (E.5)$$

$$u_{ij} = \min\{\Phi^{-1}(\tau_{ij}^u), \min(z_{vj}^{obs} : z_{vj}^{obs} \in \mathcal{I}_j^{q+1}, v = 1, \dots, n)\}. \quad (E.6)$$

with $\tau_{ij}^\ell, \tau_{ij}^u$ defined as in Step 1 of Algorithm 1. For binary study variables, the upper and lower truncation limits are

$$\ell_{ij} = \begin{cases} 0, & y_{ij}^{obs} = 1 \\ -\infty, & y_{ij}^{obs} = 0 \end{cases}, \quad u_{ij} = \begin{cases} \infty, & y_{ij}^{obs} = 1 \\ 0, & y_{ij}^{obs} = 0. \end{cases} \quad (\text{E.7})$$

Similarly, for missingness indicators, the upper and lower truncation limits are

$$\ell_{ij} = \begin{cases} 0, & r_{ij} = 1 \\ -\infty, & r_{ij} = 0 \end{cases}, \quad u_{ij} = \begin{cases} \infty, & r_{ij} = 1 \\ 0, & r_{ij} = 0. \end{cases} \quad (\text{E.8})$$

Finally, for unordered categorical variables augmented with the diagonal orthant representation of Section D, the upper and lower truncation limits for each component of \mathbf{z}_{ij} are

$$\ell_{ijc} = \begin{cases} 0, & \gamma_{ijc} = 1 \\ -\infty, & \gamma_{ijc} = 0 \end{cases}, \quad u_{ijc} = \begin{cases} \infty, & \gamma_{ijc} = 1 \\ 0, & \gamma_{ijc} = 0. \end{cases} \quad (\text{E.9})$$

4. Sample \tilde{F}_j

For each unique $\{y_j^q\}_{j=1}^{s_j}$, we first find $Z_j(y_j^q)$ as defined in the main text and compute

$$\tilde{F}_j(y_j^q) = \Phi_j\{Z_j(y_j^q)\}. \quad (\text{E.10})$$

Here, Φ_j is the Gaussian CDF for Z_j under the current draw of copula parameters. To estimate \tilde{F}_j across unobserved values, we fit a monotone interpolating spline to $\{y_j^q\}_{q=1}^{s_j} \cup \mathcal{A}_j, \{\tilde{F}_j(y_j^q)\}_{q=1}^{s_j} \cup \{\tau_j^q\}_{q=1}^{\ell_j}$ as described in Section 3.2 of the main text, and use this estimate to approximate $\tilde{F}_j(x')$ for $x' \notin \{y_j^q \cup \mathcal{A}_j\}$.

The smoothing step in the sampling of \tilde{F}_j is needed for multiple imputation, as the transformation $y_{ij}^{mis} = \tilde{F}_j^{-1}(z_{ij}^{mis})$ provides realizations across the entire support of Y_j .

We now describe how to modify these steps for the EQL. The sampling of latent variables corresponding to observed numeric (ordered discrete and continuous) variables, and specifically the lower and upper bounds in (E.5) and (E.6), are now given by $\tau^\ell = \max\{F_j^{-1}(\tau_j^q) \in \mathcal{A}_j : y_{ij} > F_j^{-1}(\tau_j^q)\}$ and $\tau^u = \min\{F_j^{-1}(\tau_j^q) \in \mathcal{A}_j : y_{ij} < F_j^{-1}(\tau_j^q)\}$, since we no longer have intermediate quantile points. In addition, the interpolation step for F_j smooths between pairs $[\mathcal{A}_j, \{\tau_j^q\}_{q=1}^{\ell_j}]$ since we no longer compute (E.10).

F Additional Simulation Results

This section includes supporting results for the some of the statements made in Section 4.1 of the main text.

F.1 Accuracy with Sparse Auxiliary Information

Fixing $p = 10$ study variables and the proportion of marginal missingness at 50%, we now provide comparisons of the efficiency of posterior inference for the copula correlation by gradually increasing the set of auxiliary quantiles incorporated into the model. In Figure F.1, we include the same plots as the main text, augmented with inference under the auxiliary sets comprising every fourth quantile (i.e., $\mathcal{A}_j = \{0, 0.04, 0.08, \dots, 1\}$) and every decile (i.e., $\mathcal{A}_j = \{0, 0.1, 0.2, \dots, 1\}$). We observe small gains when increasing the number of true auxiliary quantiles introduced for each margin. However, as the sample size increases, the gains become practically negligible relative to using Median or MA + Median.

We also check whether the results are sensitive to the dimension of the study variables. Figure F.2 increases the dimension of the study variables to $p = 20$, holding the missingness at 50%. The results show similar patterns as Figure 3 in the main text, owing to the scalability of the factor model used to model the latent variables. We do not include the RL of (Hoff, 2007) in these comparisons because the computation is infeasible with our setup when $p = 20$ and $n > 1000$. For $p = 5$, the RL copula sampler took nearly 4

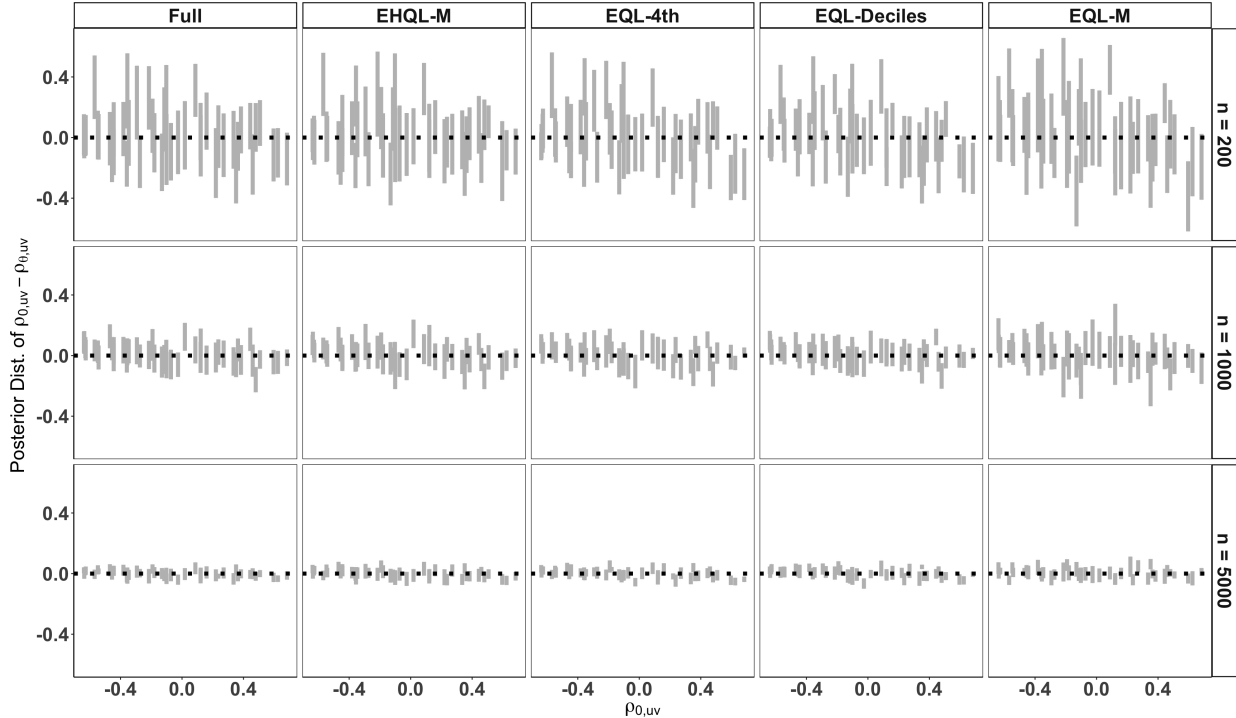


Figure F.1: Expanding Figure 3 in the main text to all levels of auxiliary information considered in the simulation study. Minor gains for smaller sample sizes are observed by incorporating more auxiliary quantiles into the model relative to using just the median. Even with every fourth quantile, the inferences are virtually indistinguishable from the MA + median method.

hours to complete for $n = 5000$. By contrast, with $n = 5000$ and $p = 20$ study variables, the EQL/EHQL completed 10000 iterations in around 15 minutes on average using a 2023 Macbook Pro. The computation could be sped up with parallel computing for the sampling of \mathbf{z} , since the columns are conditionally independent under the factor model. We leave this to future research.

Finally, we complete the information in Figure 4 in the main text by lowering the missingness to 25% and plotting posterior samples of the interpolated marginals obtained using Algorithm 2 in the main text. As shown in Figure F.3, the interpolation accurately captures notable features of each distribution function, with minor gains under less severe missingness, particularly for smaller sample sizes. These findings are not sensitive to the type of F_j or p .

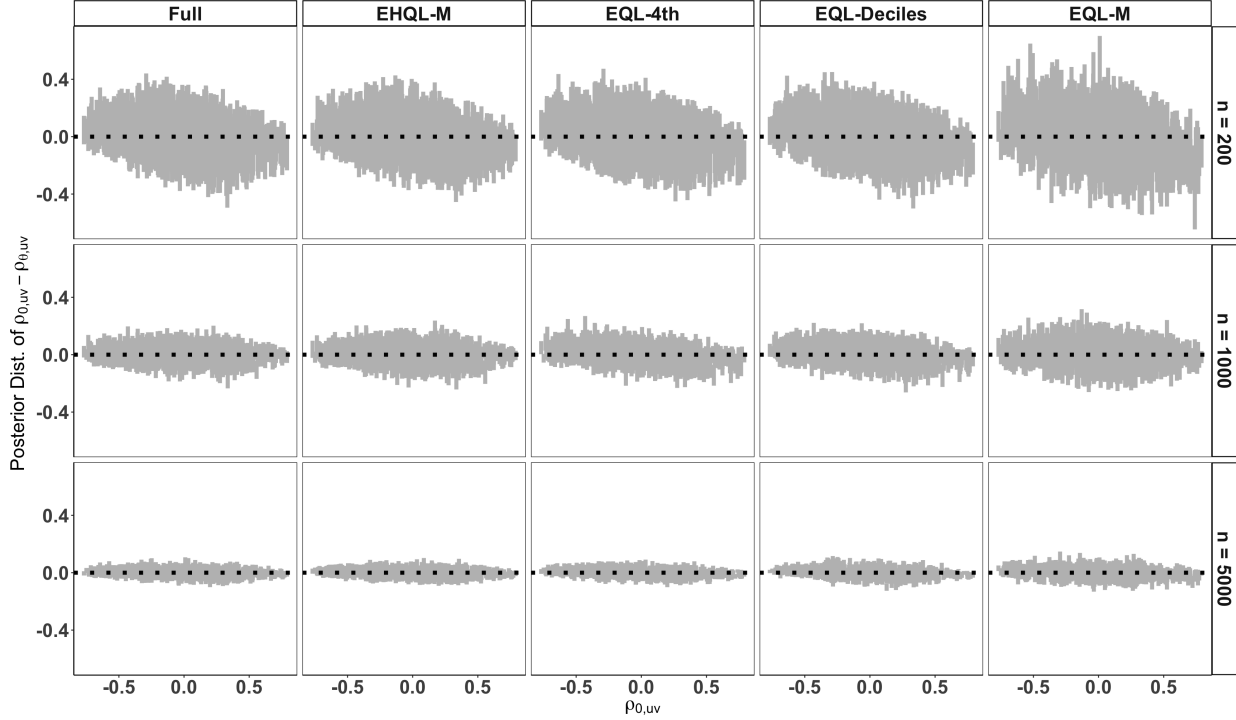


Figure F.2: Results of the simulation using $p = 20$ study variables. As in the main paper, the contraction of the posterior is moderately impacted by the level of auxiliary information introduced in the model, particularly for smaller sample sizes. This is evidenced by the interval widths for EQL-M, which are wider than those for the other auxiliary specifications.

F.2 Simulation of Repeated Sampling Performance

In the main text, we summarise the improvement of the EHQL copula over MICE in empirical coverage rates under the repeated sampling experiment. We mention that the average interval widths are similar, and so the gains are not merely due to wider uncertainty under the proposed approach. We support this claim in Figure F.4, which plots the average confidence interval widths for the quantile regression coefficients across the experiment. The results for the other settings considered are consistent.

In Section 4.2 of the main text, we specified the median as the additional auxiliary quantile for NDI to the lower and upper bounds. Here, we repeat the simulation in Section 4.2 of the main text using the auxiliary 75th quantile for NDI in addition to lower and upper bounds. As shown in Figure F.5, the results are consistent with what is presented in the main text.

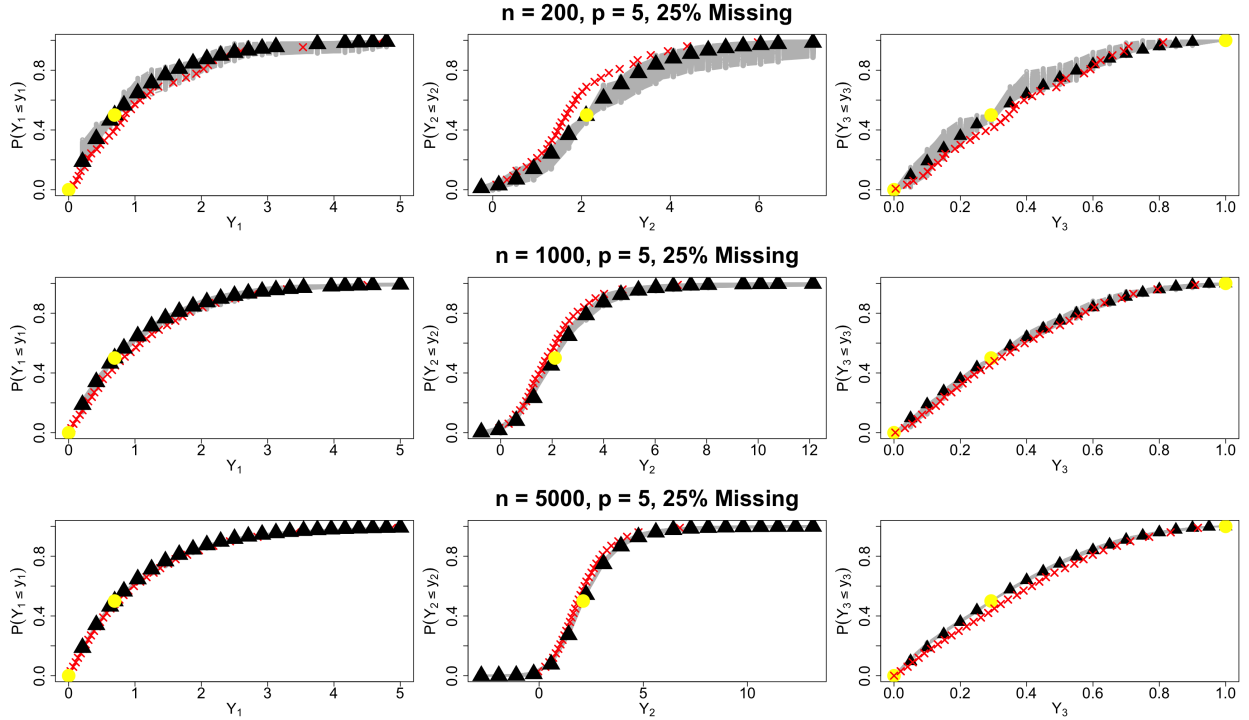


Figure F.3: The same comparisons as Figure 4 in the main text, but now with 25% marginal missingness. Since there is only 25% missingness, the ECDF is less biased. Again, the interpolation strategy at intermediate quantile points enables accurate estimation of each marginal, which holds for each study variable.

The EHQL copula outperforms MICE on multiple imputation inferences for all quantile regression coefficients corresponding to NDI.

We also include results from misspecifying the auxiliary quantile introduced into the model. To do so, we set $\mathcal{A}_{\text{NDI}} = \{F^{-1}(0), F_j^{-1}(0.5) + \epsilon, F_j^{-1}(1)\}$, $\epsilon \in \{0.5, 1\}$. That is, we increasingly perturb the true median for NDI. Figure F.6 displays the results. As expected, the performance of the EHQL copula model deteriorates as the auxiliary quantiles are increasingly biased. However, the performance still improves upon MICE for $\epsilon = 0.5$.

G Analysis of North Carolina Data: Additional Results

In this section, we provide details on the auxiliary information from the CDC used in \mathcal{A} , posterior predictive checks of the Gaussian copula model on the observed data, and additional quantile regression inferences not presented in the main text.

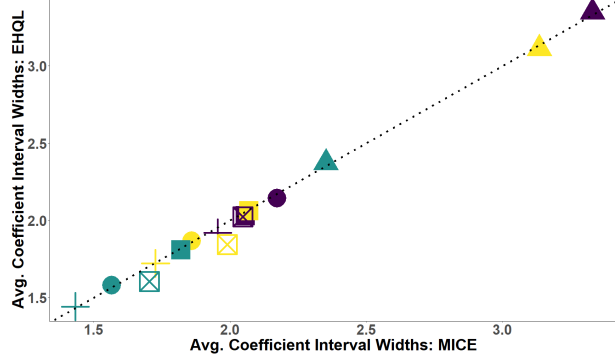


Figure F.4: Average interval widths of multiple imputation confidence intervals for the EHQL copula and MICE. Results are presented for the auxiliary specification presented in the main text (i.e., the median for NDI is incorporated into the copula model). The gains in empirical coverage rates under the proposed approach are not simply due to wide confidence intervals

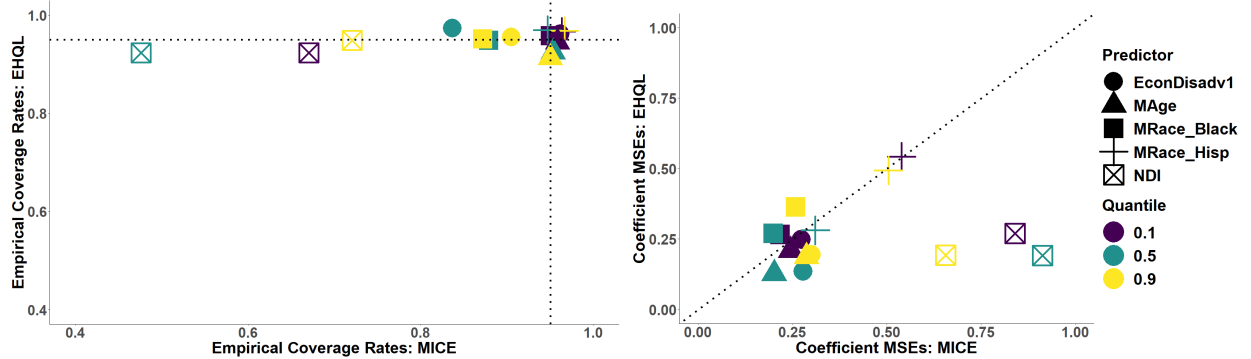


Figure F.5: Empirical coverage rates (left) and average mean squared error (MSE) of multiple imputation point estimates for the EHQL copula and MICE imputations in the repeated simulation study. Instead of specifying the median for NDI, we use the 75th population quantile (in addition to the upper and lower bounds) as the auxiliary information set. Both approaches perform similarly for coefficients other than NDI, which is subject to nonignorable missingness. For this coefficient, the EHQL provides lower bias and higher coverage.

G.1 Determining Auxiliary Information from CDC Estimates

As mentioned in Section 5 of the main text, we leverage published quantile estimates of lead exposure from the CDC (Centers for Disease Control and Prevention, 2022) to specify auxiliary quantiles on blood-lead levels. Table G.1 displays the population-level estimates provided by the CDC. Among the children in the North Carolina data who were measured for lead, 90% were measured between 2005 and 2009. Since they were born between 2003 and 2005, we base the auxiliary information \mathcal{A} on the published estimates between 2005 and

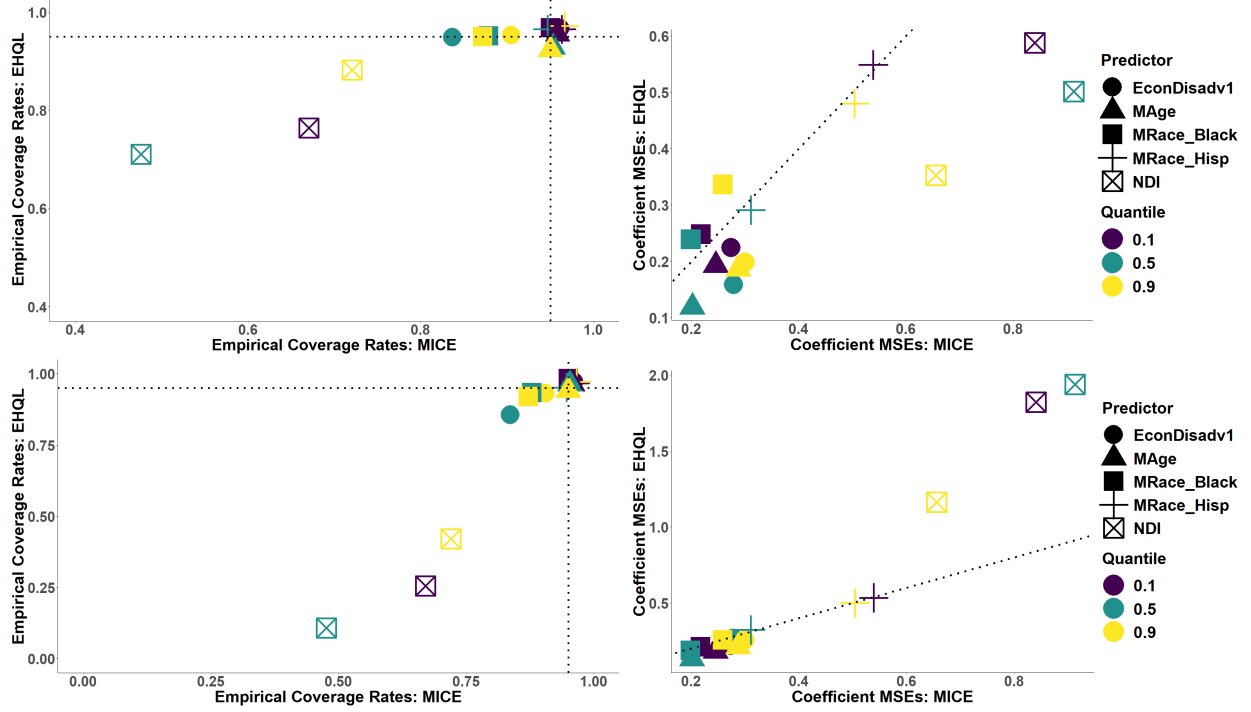


Figure F.6: Empirical coverage rates (left column) and average mean squared error of multiple imputation point estimates (right column) for the EHQL copula and MICE imputations in the repeated simulation study. Here, we misspecify the auxiliary median for NDI by $\epsilon = 0.5$ (top row) and $\epsilon = 1$ (bottom row). For $\epsilon = 0.5$, the EHQL still performs better than MICE in inference for the quantile regression coefficients of NDI. However, with extreme misspecification, the EHQL copula does not offer reliable inferences under nonignorable missing data.

2010 for the 1-5 years old group.

We incorporate a single auxiliary quantile (besides the lower and upper bounds) for two reasons. First, the CDC estimates are continuous, whereas the North Carolina data are binned into intervals of exposure. For instance, observing `Blood_lead = 1` implies that an individual has a measure between $(0, 1] \mu\text{g}/\text{ml}$. Second, the reported quantiles are national estimates, whereas we use data from North Carolina.

G.2 Posterior Predictive Checks

We verify that the EHQL copula model generates predictive samples that resemble plausible realizations of the observed values in the North Carolina lead exposure data. Specifically, we examine the joint predictive distribution of `Blood_lead` and the other study variables

Demographic Categories	Survey (Years)	Geometric Mean (95% CI)	50th Percentile (95% CI)	75th Percentile (95% CI)	90th Percentile (95% CI)	95th Percentile (95% CI)	Sample Size
Total population	99-00	1.66 (1.60-1.72)	1.60 (1.60-1.70)	2.50 (2.40-2.60)	3.80 (3.60-4.00)	5.00 (4.70-5.50)	7970
Total population	01-02	1.45 (1.39-1.51)	1.40 (1.40-1.50)	2.20 (2.10-2.30)	3.40 (3.20-3.60)	4.50 (4.20-4.70)	8945
Total population	03-04	1.43 (1.36-1.50)	1.40 (1.30-1.50)	2.10 (2.10-2.20)	3.20 (3.10-3.30)	4.20 (3.90-4.40)	8373
Total population	05-06	1.29 (1.23-1.36)	1.27 (1.20-1.34)	2.01 (1.91-2.11)	3.05 (2.86-3.22)	3.91 (3.64-4.18)	8407
Total population	07-08	1.27 (1.21-1.34)	1.22 (1.18-1.30)	1.90 (1.80-2.00)	2.80 (2.67-2.96)	3.70 (3.50-3.90)	8266
Total population	09-10	1.12 (1.08-1.16)	1.07 (1.03-1.12)	1.70 (1.62-1.77)	2.58 (2.45-2.71)	3.34 (3.14-3.57)	8793
Age 1-5 years	99-00	2.23 (1.96-2.53)	2.20 (1.90-2.50)	3.40 (2.80-3.90)	4.90 (4.00-6.60)	7.00 (6.10-8.30)	723
Age 1-5 years	01-02	1.70 (1.55-1.87)	1.60 (1.50-1.80)	2.50 (2.20-2.90)	4.20 (3.50-5.20)	5.80 (4.70-6.90)	898
Age 1-5 years	03-04	1.77 (1.60-1.95)	1.70 (1.50-1.90)	2.50 (2.30-2.80)	3.90 (3.30-4.60)	5.10 (4.10-6.60)	911
Age 1-5 years	05-06	1.46 (1.36-1.57)	1.43 (1.34-1.55)	2.10 (1.97-2.20)	2.98 (2.72-3.32)	3.80 (3.49-4.54)	968
Age 1-5 years	07-08	1.51 (1.37-1.66)	1.43 (1.30-1.60)	2.20 (1.98-2.31)	3.20 (2.65-3.85)	4.10 (3.40-5.19)	817
Age 1-5 years	09-10	1.17 (1.08-1.26)	1.15 (1.03-1.27)	1.70 (1.50-1.87)	2.39 (2.08-2.65)	3.37 (2.63-4.11)	836
Age 6-11 years	99-00	1.51 (1.36-1.66)	1.40 (1.30-1.60)	2.10 (1.80-2.50)	3.30 (2.80-3.80)	4.50 (3.40-6.20)	905
Age 6-11 years	01-02	1.25 (1.14-1.36)	1.20 (1.00-1.30)	1.70 (1.60-2.00)	2.80 (2.50-3.10)	3.70 (3.00-4.70)	1044
Age 6-11 years	03-04	1.25 (1.12-1.39)	1.20 (1.10-1.40)	1.80 (1.50-2.10)	2.60 (2.10-3.10)	3.30 (2.50-4.60)	856
Age 6-11 years	05-06	1.02 (0.98-1.10)	.970 (.890-1.01)	1.40 (1.28-1.55)	2.06 (1.80-2.72)	3.00 (2.26-3.81)	934
Age 6-11 years	07-08	.988 (914-1.07)	.960 (.880-1.07)	1.31 (1.22-1.49)	1.90 (1.70-2.11)	2.50 (2.10-2.88)	1011
Age 6-11 years	09-10	.838 (.792-887)	.810 (.740-840)	1.13 (1.06-1.21)	1.64 (1.45-1.84)	2.01 (1.88-2.25)	1009

Figure G.1: CDC published estimates for select quantiles of lead exposure.

given that `Blood_lead` is observed.

Given a posterior draw of $\{\mathbf{C}_\theta, \boldsymbol{\alpha}, \{\tilde{F}_j\}\}$, we can generate replicate values of \mathbf{y}^{obs} in three steps. Let $j = 1$ when Y_j is `Blood_lead`. We generate the predictive latent variables corresponding to lead exposure being observed, i.e., $\tilde{z}_{r_1} \sim N(\alpha_{r_1}, 1)\mathbb{1}_{(-\infty, 0)}$. We then generate predictive latent variables for the study variables conditional on the sampled \tilde{z}_{r_1} using the distribution for $\tilde{\mathbf{z}}_y \mid \tilde{z}_{r_1}$. This is conditionally multivariate Gaussian with the mean varying as a function of the realized \tilde{z}_{r_1} and covariance $\boldsymbol{\Sigma}^*$ derived from \mathbf{C}_θ . For each numeric Y_j , for a hypothetical individual i we obtain $\tilde{y}_{ij} = \tilde{F}_j^{-1}(\Phi(\tilde{z}_{ij}))$. For binary variables, sampling $\tilde{z}_{ij} > 0$ indicates for our hypothetical individual that $\tilde{y}_{ij} = 1$. For Y_j that is unordered categorical, we generate the vector $\tilde{\mathbf{z}}_{ij}$, and set $\tilde{Y}_{ij} = c \iff \tilde{z}_{ijc} = \max\{\tilde{z}_{ij}\}$. We repeat this process ten times per parameter draw, resulting in 50,000 posterior predictive samples.

We note here that our posterior predictive sampling of the categorical variables does not enforce the diagonal orthant restriction of Section D as part of the latent variable generation; rather, for any y_{ij}^{mis} , we generate its value by selecting the c corresponding to the maximum value in $\{z_{ijc} : c = 1, \dots, c_j\}$. This is done for computational convenience. To enforce it, we would have to decompose the joint distribution of the latent study variables into a sequence of conditionals for each \mathbf{z}_{ij} corresponding to an unordered categorical variable. Then, we would compute the mean and variance, derive the categorical probabilities, and sample a multinomial. The resulting categorical membership would specify the diagonal orthant set

restriction for those variables, after which predictive latent variables could be sampled.

To compute Σ^* , we first partition each posterior sample of

$$\mathbf{C}_\theta = \begin{bmatrix} \mathbf{C}_y & \mathbf{C}_{yr} \\ \mathbf{C}_{ry} & \mathbf{C}_r \end{bmatrix}. \quad (\text{G.1})$$

Then, $\Sigma^* = \mathbf{C}_y - \mathbf{C}_{yr}\mathbf{C}_r^{-1}\mathbf{C}_{ry}$.

Figure G.2 displays the joint predictive distribution of reading/math scores and blood-lead levels. Table 1 compares the posterior predictive means of `Blood_lead` ($\bar{Y}_{\text{blood_lead}}^{\text{pred}}$) for each level of the binary/categorical variables in the model with their counterparts in the observed data. Table 2 compares the correlations between $\tilde{Y}_{\text{blood_lead}}$ of the remaining numeric variables in the predictive samples and observed data. We see some evidence of lack of fit for average lead levels for Hispanic children, who represent less than 10% of the observations. Nonetheless, overall, the copula model adequately captures the associations in the observed data. All results are for the EHQL copula with auxiliary `Blood_lead` quantile $F(2) = 0.75$.

	mRace (Wh./Bl./Hisp.)	mEduc (No H.S., H.S., Coll.)	EconDisadv (No/Yes)	Male (No/Yes)	NotMarried (No/Yes)	Smoker (No/Yes)
$\bar{Y}_{\text{Blood_lead}}^{\text{pred}}$	2.68/3.28/2.92	3.20/2.98/2.38	2.49/3.13	2.82/2.92	2.58/3.25	2.80/3.23
$\bar{Y}_{\text{Blood_lead}}^{\text{obs}}$	2.65/3.16/2.59	3.07/2.84/2.31	2.46/3.02	2.74/2.85	2.58/3.05	2.75/3.07

Table 1: Posterior predictive means of `Blood_lead` compared to observed means by each level of the categorical and binary study variables. The EHQL copula model accurately captures these multivariate associations in the observed data.

Yj	mAge	NDI	RI	BWTpct	Gestation
$\text{cor}(Y_j, \text{Blood_lead})^{\text{pred}}$	-0.12	0.22	0.11	-0.03	0.03
$\text{cor}(Y_j, \text{Blood_lead})^{\text{obs}}$	-0.14	0.15	0.12	-0.07	-0.001

Table 2: Predictive correlations compared to observed correlations between `Blood_lead` and the other numeric study variables, excluding reading and math scores. The EHQL copula approximately captures these pairwise associations in the observed data.

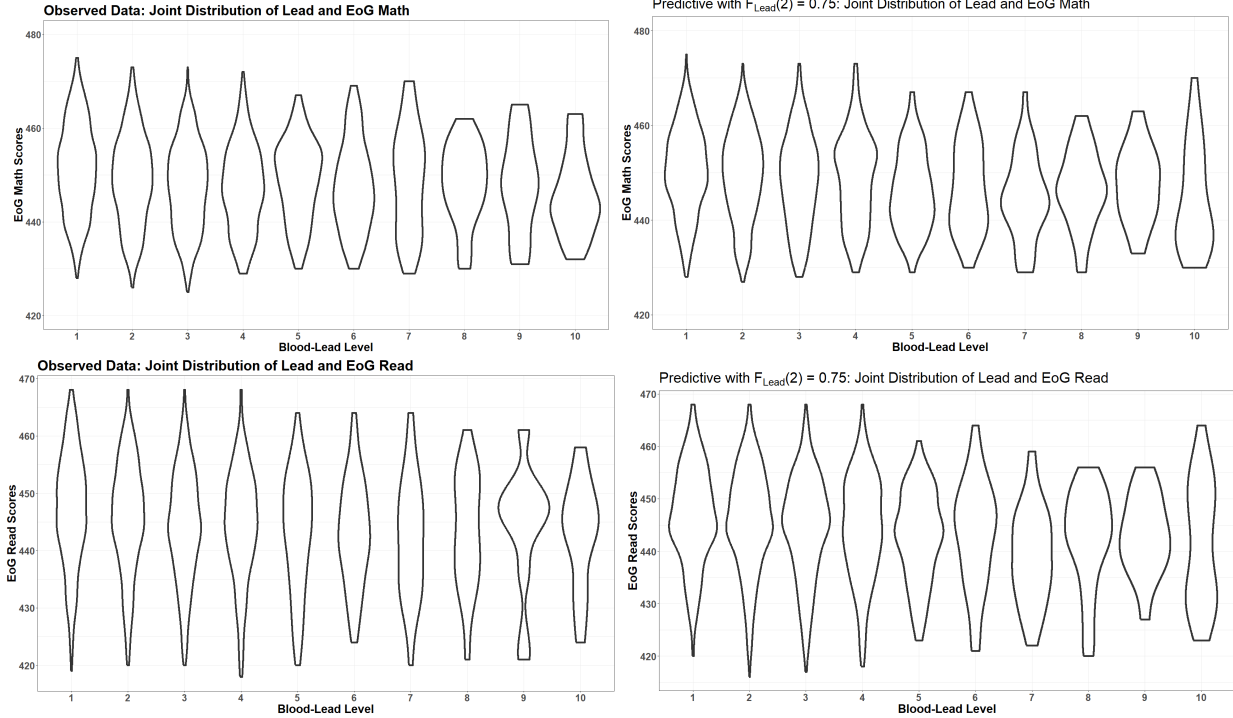


Figure G.2: Observed (left column) vs posterior predictive (right column) distributions of math/reading EoG test scores and blood-lead levels. The EHQL copula model adequately captures the bivariate associations between the EoG test scores and lead exposure.

G.3 Complete Results for the 10th Quantile Regression

In the main paper, we present results for the 10th quantile regression coefficients for selected exposure variables using EoG math scores as the response. In this section we provide the multiple imputation coefficient estimates and 95% confidence intervals for the remaining coefficients, and also include parallel results using EoG reading scores as the response. Here, $F_{\text{Blood_lead}}(2) = 0.75$.

Figure G.3 provides the multiple imputation inferences for the remaining coefficients with EoG math scores as the response variable. Both the EHQL and MICE provide inferences that are notably different than complete cases (CC) analysis. Unsurprisingly, the inferences from both approaches are very similar, as these variables are almost completely observed and both the EHQL and MICE treat their missingness as MCAR.

Figure G.4 presents multiple imputation inferences for the 10th quantile regression for the

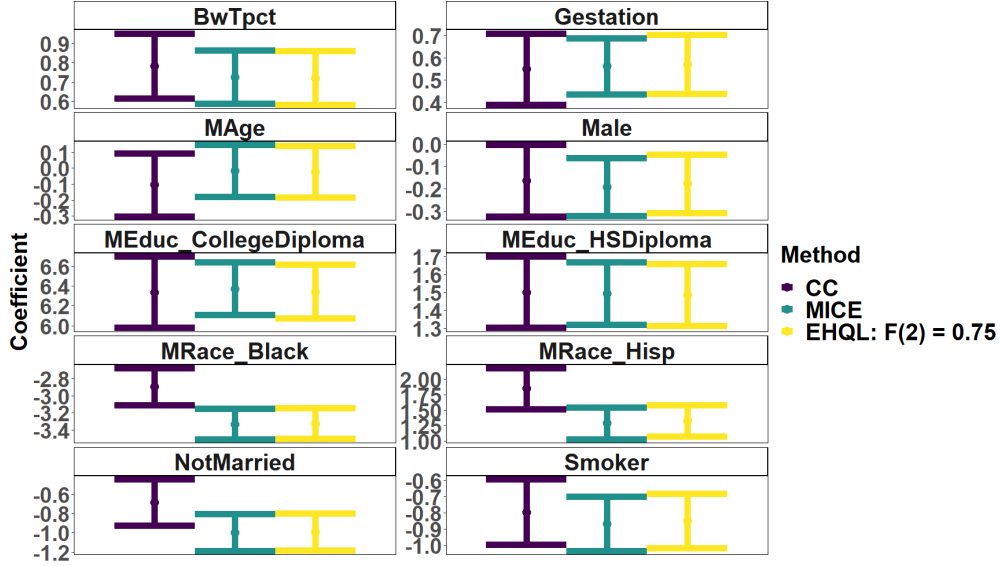


Figure G.3: Multiple imputation inferences for the remaining coefficients under the 10th quantile regression. Here, $F_{\text{Blood_lead}}(2) = 0.75$ and the response variable is EoG math scores. For both the EHQL and MICE, multiple imputation offers more precision and shifts certain coefficients relative to CC analysis. The inferences between the two methods are virtually identical, owing the fact that the variables are almost completely observed and we treat their missingness as MCAR.

four selected exposure variables presented in the main text with EoG reading test scores as the response. Accounting for the nonignorable missingness in lead exposure measurements still results in stronger, more adverse associations for reading test scores and lead exposure, although the shift is not as pronounced as for math test scores. As with the quantile regressions using math test scores as the dependent variable, we see little practical difference between the EHQL and MICE results for the three coefficients that do not correspond to `Blood_lead`.

Finally, Figure G.5 displays multiple imputation inferences for the remaining coefficients with EoG reading test scores as the response. The multiple imputation inferences result in greater precision. The EHQL and MICE offer very similar inferences—which are sometimes quite different than the CC inferences—due to the dearth of missing values for these other variables.

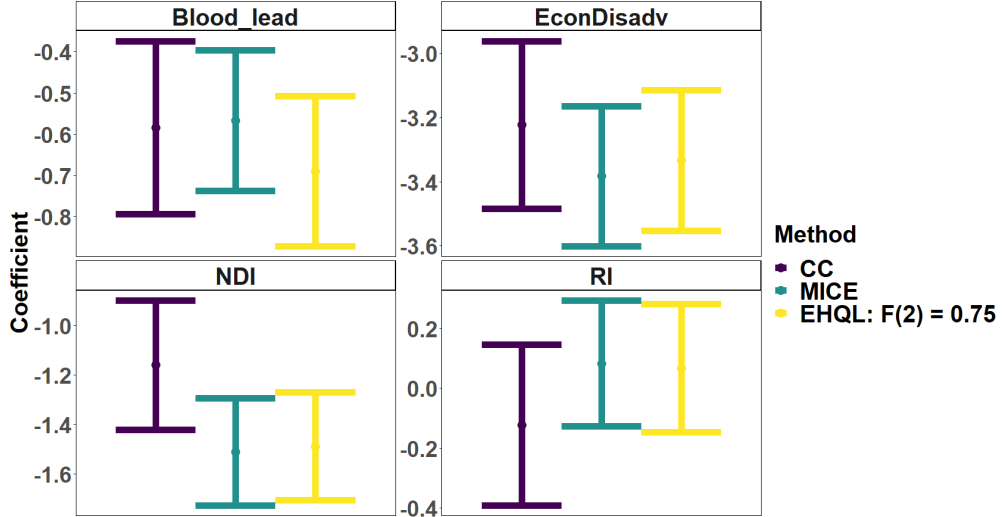


Figure G.4: Multiple imputation inference for the remaining coefficients under the 10th quantile regression. Here, $F_{\text{Blood_lead}}(2) = 0.75$ and the response variable is EoG reading scores. Similar to the model with EoG math scores as the response, the EHQL estimates a more strong, adverse association between lead exposure and reading scores than both CC and MICE.

G.4 Results from Additional Quantile Regressions and Alternative Auxiliary Quantile Specifications

In this section, we demonstrate that the quantile regression inferences are not sensitive to the alternative auxiliary specifications considered ($F_{\text{Blood_lead}}(2) = 0.80$, $F_{\text{Blood_lead}}(2) = 0.70$). We combine these with results for the quantile regressions at the 50th and 90th quantiles, when either EoG math or reading test scores is the response variable. To economize on the number of figures, we present the results for all quantile regressions and auxiliary specifications in the same plots. We again distinguish between the four selected exposure variables and the remaining covariates.

Figures G.6 and G.7 provide results for the models with EoG math scores as the response, and Figures G.8 and G.9 provide results for the models with EoG reading scores as the response. Across all analyses, we see little differences in the inferences for these different specifications of the auxiliary quantile, suggesting the results are not sensitive to modest perturbations of the auxiliary quantile specification. Accounting for the nonignor-

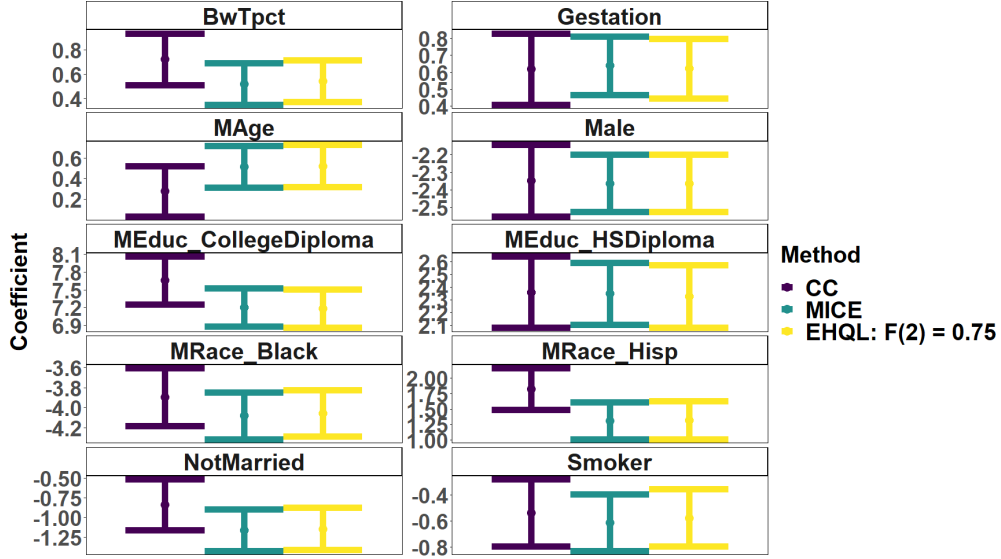


Figure G.5: Multiple imputation inference for the remaining coefficients under the 10th quantile regression. Here, $F_{\text{Blood_lead}}(2) = 0.75$ and the response variable is EoG reading scores. For both the EHQL and MICE, imputation offers more precision and shifts certain coefficients relative to CC analysis. The inferences between the two methods are virtually identical, owing the fact that the variables are almost completely observed and we treat their missingness as MCAR.

able missingness in `Blood_lead` seems to have greater effects on the inferences for the math regressions than for the reading regressions. The effects of lead exposure appear relatively constant across quantiles for the math regressions, whereas they are more adverse at lower quantiles for the reading regressions.

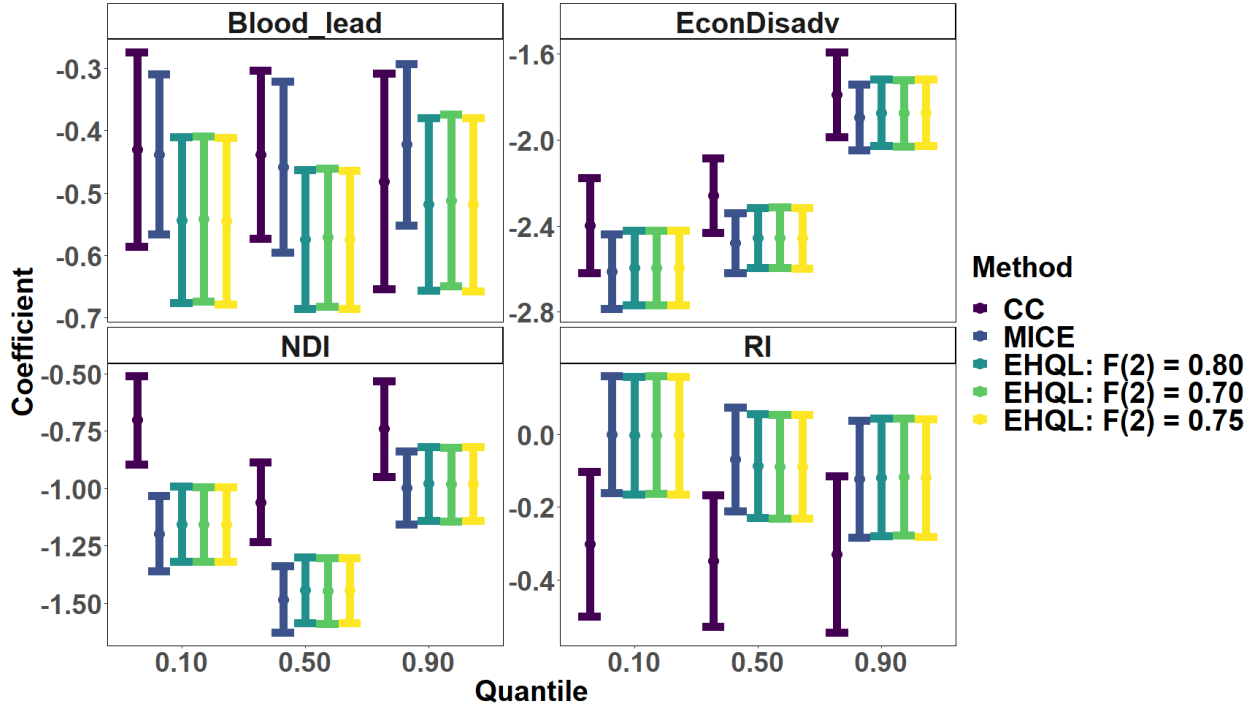


Figure G.6: Multiple imputation inferences for quantile regression coefficients for the four predictors highlighted in the main text for all quantile regressions and auxiliary quantile settings. EoG math test score is the response variable. We observe that inference is not sensitive to auxiliary quantile specifications for lead exposure under the proposed approach, with sizeable shifts between complete case (CC) inference for all coefficients across quantiles. Furthermore, for each auxiliary quantile specification and quantile regression, Blood_lead is more adversely associated with EoG math scores than it is in both the CC and MICE inferences.

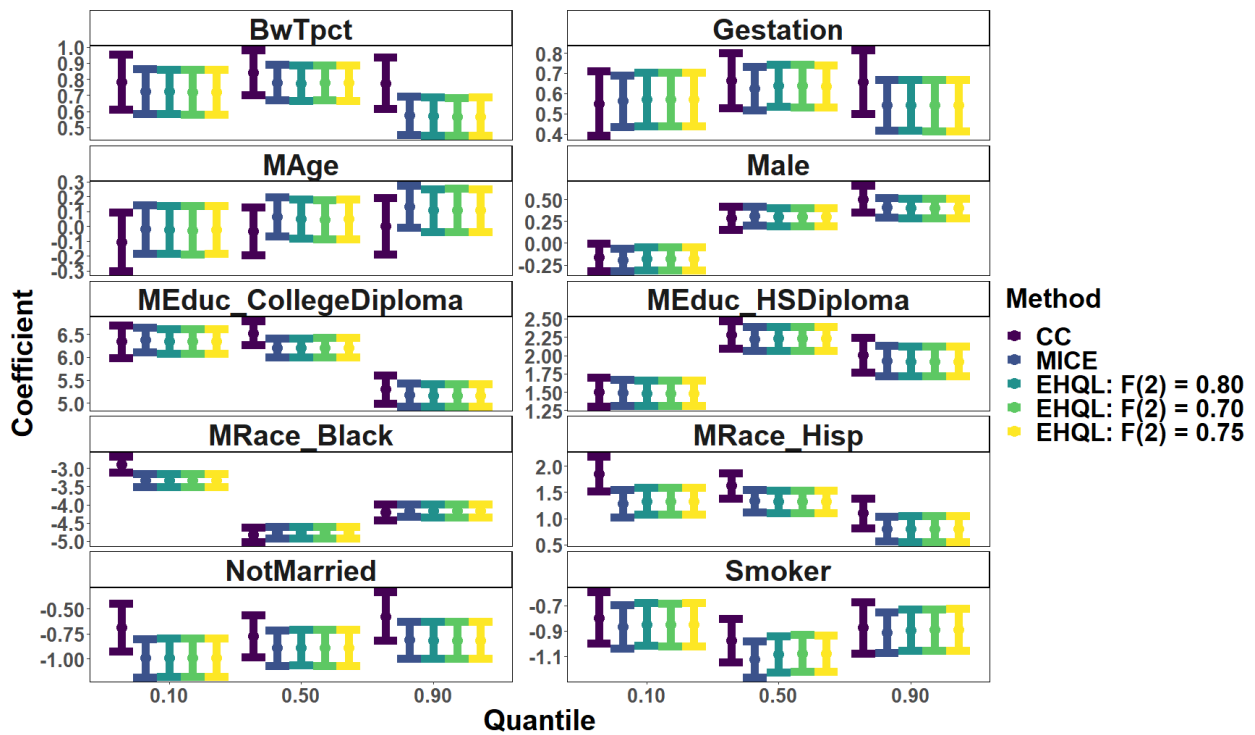


Figure G.7: Multiple imputation inferences for quantile regression coefficients for the remaining covariates in the analysis of the North Carolina lead exposure data presented in the main text. EoG math test score is the response variable.

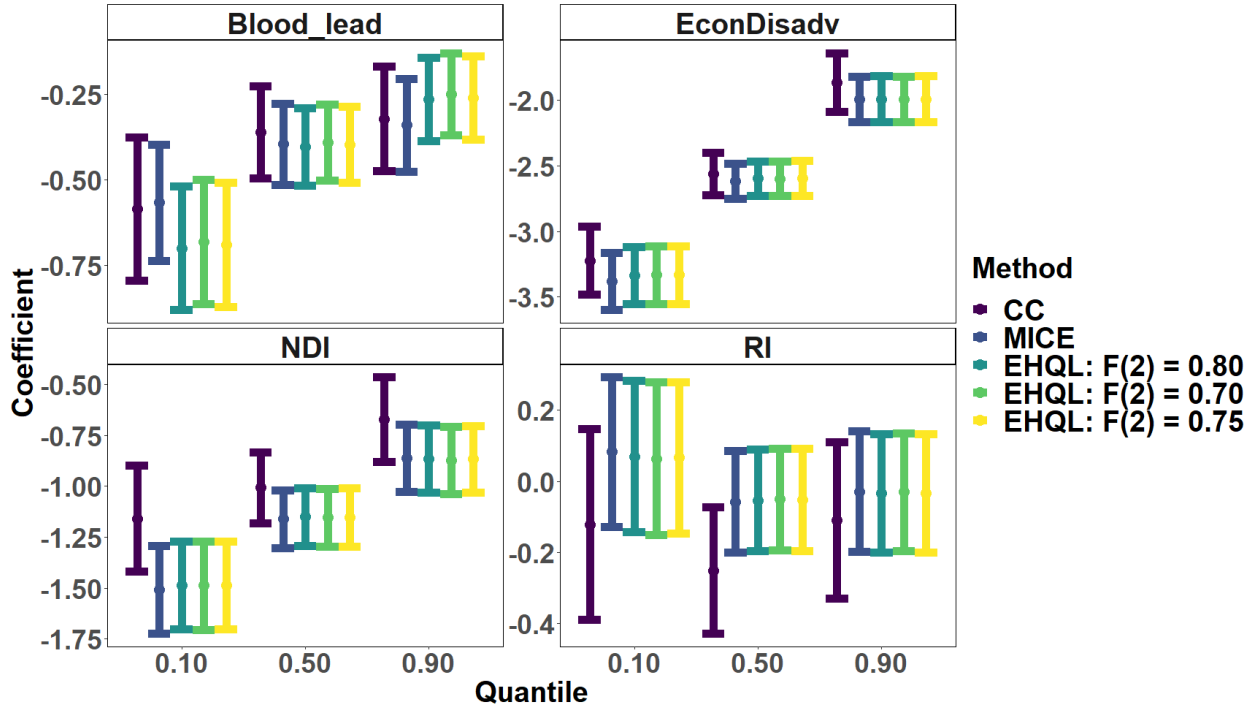


Figure G.8: Multiple imputation inferences with EoG reading test score as the response variable. Results are for the quantile regression coefficients for the four predictors highlighted in the main text for all quantile regressions and auxiliary quantile settings. For EoG reading scores, the imputations under the EHQL copula suggest more heterogeneous impacts of *Blood_lead* across the distribution of reading scores. This includes estimating a more adverse impact of lead for lower scoring children. By contrast, the MICE imputations estimate the quantile regression coefficients as closer to one another.

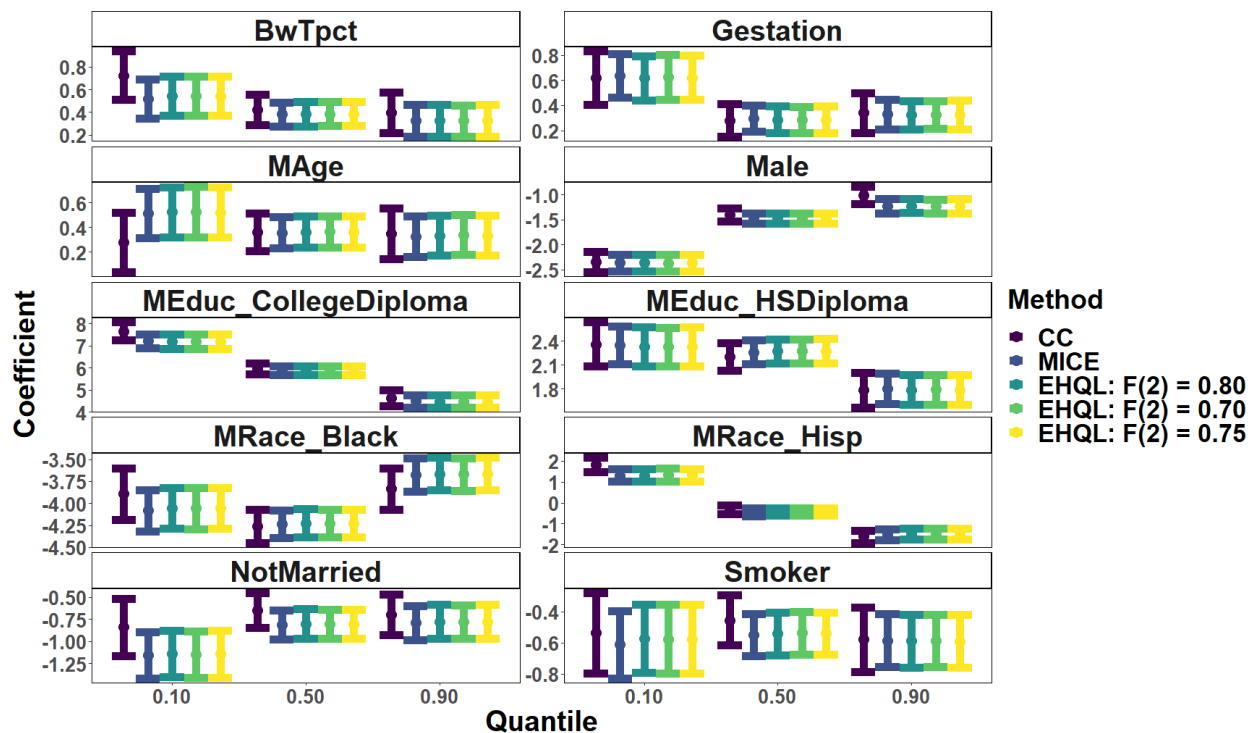


Figure G.9: Multiple imputation inferences with EoG reading test score as the response variable for the remaining coefficients.

References

Arellano-Valle, R. B. and Azzalini, A. (2006). On the unification of families of skew-normal distributions. *Scandinavian Journal of Statistics*, 33:561–574.

Bhattacharya, A. and Dunson, D. B. (2011). Sparse Bayesian infinite factor models. *Biometrika*, 98:291–306.

Centers for Disease Control and Prevention (2022). CDC Exposure Report Data Tables. https://www.cdc.gov/exposurereport/data_tables.html.

Feldman, J. and Kowal, D. R. (2022). Bayesian data synthesis and the utility-risk trade-off for mixed epidemiological data. *The Annals of Applied Statistics*, 16:2577–2602.

Gu, J. and Ghosal, S. (2009). Bayesian ROC curve estimation under binormality using a rank likelihood. *Journal of Statistical Planning and Inference*, 139(6):2076–2083.

Hoff, P. D. (2007). Extending the rank likelihood for semiparametric copula estimation. *The Annals of Applied Statistics*, 1:265–283.

Johndrow, J., Dunson, D., and Lum, K. (2013). Diagonal orthant multinomial probit models. In *Artificial Intelligence and Statistics*, pages 29–38. PMLR.

Miller, J. W. (2021). Asymptotic normality, concentration, and coverage of generalized posteriors. *Journal of Machine Learning Research*, 22:1–53.

Olsson, U. (1979). Maximum likelihood estimation of the polychoric correlation coefficient. *Psychometrika*, 44:443–460.

Sadinle, M. and Reiter, J. P. (2019). Sequentially additive nonignorable missing data modelling using auxiliary marginal information. *Biometrika*, 106:889–911.